DEPARTMENT OF TRANSPORTATION

Harnessing Solar Energy through Solar Snow Fence: Implementation

Mijia Yang, Principal Investigator
Department of Civil, Construction and Environmental Engineering
North Dakota State University

May 2025

Research Report
Final Report 2025-25

To get this document in an alternative format or language, please call 651-366-4720 (711 or 1-800-627-3529 for MN Relay). You can also email your request to ADArequest.dot@state.mn.us. Please make your request at least two weeks before you need the document.

Technical Report Documentation Page

1. Report No.	2.	3. Recipients Accession No.
MN 2025-25		

4. Title and Subtitle	5. Report Date
Harnessing Solar Energy through Solar Snow Fence: Implementation	May 2025
	6.

7. Author(s)	8. Performing Organization Report No.
Mijia Yang, Yao Yu, Qifeng Zhang	

9. Performing Organization Name and Address	10. Project/Task/Work Unit No.
Department of Civil, Construction and Environmental Engineering North Dakota State University 1410 14th Ave N, Fargo, ND 58104	11. Contract (C) or Grant (G) No. (c)1036338 (wo) 4

12. Sponsoring Organization Name and Address	13. Type of Report and Period Covered
Minnesota Department of Transportation Office of Research & Innovation 395 John Ireland Boulevard, MS 330 St. Paul, Minnesota 55155-1899	Final Report
	14. Sponsoring Agency Code

15. Supplementary Notes

http://mdl.mndot.gov/

16. Abstract:

A 100-ft field implementation of the proposed solar snow fence was conducted In Glyndon, MN. The implementation process started with the manufacturing of solar stripe frames, U connection with steel posts, helical piling, electrical power harvest and storage, electrical use in snow melting, and monitoring of the solar snow fence systems. A 12-ft lab prototype was first built, and verification of the monitoring sensors and the efficiency of the solar snow fence has been completed. All the sensors have reached more than 95% accuracy and an average of 829 W power was produced through the 12-ft prototype. The full 100-ft solar snow fence assembly and field construction were completed in August 2023. In the past 18 months, the solar snow fence has proven to work well with different ambient conditions, and the temperature, moisture, wind speed, solar intensity, electrical voltage, and current have been collected. The correlation between the solar intensity and the power harvested has been created, and an average of 11-25 kW*h energy has been produced daily. The energy produced has been used to melt snow effectively.

17. Document Analysis/Descriptors	18. Availability Statement
Snow fences, Snow and ice control, Solar energy, Melting	No restrictions. Document available from: National Technical Information Services, Alexandria, Virginia 22312

19. Security Class (this report)	20. Security Class (this page)	21. No. of Pages	22. Price
Unclassified	Unclassified	89	

Harnessing Solar Energy through Solar Snow Fence: Implementation

Final Report

Prepared by:

Mijia Yang
Yao Yu
Department of Civil, Construction and Environmental Engineering,
North Dakota State University

Qifeng Zhang
Department of Electrical and Computer Engineering
North Dakota State University

May 2025

Published by:

Minnesota Department of Transportation
Office of Research & Innovation
395 John Ireland Boulevard, MS 330
St. Paul, Minnesota 55155-1899

Acknowledgements

The report's authors express appreciation to the Minnesota Department of Transportation (MnDOT) for providing the financial support to conduct this study. The authors would like to acknowledge the contribution of members of the Technical Advisory Panel (TAP) Dan Gullickson, Kohl Skalin, Kevin Chan, Jihshya Lin, Derek Olds, Peter Wasko, Susan Zarling, Kohl Skalin, and Barbara Fraley for their guidance and for facilitating the site visit and implementation of the solar snow fences. The project's TAP played a great role; the suggestions and technical feedback during TAP meetings and task-report revisions are gratefully acknowledged. The contributions of the Project Liaison Dan Gullickson, the Project Champion Kohl Skalin, and the MnDOT research office staff Barbara Fraley are greatly appreciated. The authors would also like to acknowledge the contributions of the North Dakota State University (NDSU) Civil, Construction, and Environmental Engineering Department staff, Sponsored Project Administration (SPA) staff, and the graduate and undergraduate students of NDSU's civil engineering department who helped with various project activities.

Table of Contents

List of Figures

List of Tables

List of Abbreviations

PV – Photovoltaic

PPA – Power Purchase Agreement

BOS – Balance of System

GPR – Ground Penetration Radar

AASHTO – American Association of State Highway and Transportation Officials

BDS – Bridge Design Specification

Executive Summary

MnDOT is committed to actively pursuing cost-effective energy-efficiency measures and developing solar energy-related projects. The agency acted on a previously completed phase-I project and then proposed implementing the solar snow fence project in Glyndon, MN. The objective was to test the functionalities of the solar snow fence system in an ambient condition and verify its efficiency in snow drift control and energy production.

Researchers conducted a detailed study of the holistic implementation of the solar snow fence, from solar strip frame manufacturing and assembly, helical piling, field construction, operation monitoring, snow drift data collection, and energy production monitoring.

In the solar strip frame manufacturing and assembly, an innovative T-slotted aluminum frame was used to contain the glass surfaced solar strips. A rubber gasket was used to seal the gap between the frame and the solar panel. An aluminum sliding bracket was fixed on the T-slotted aluminum frame and used to connect the steel posts. The sliding bracket could provide a 1'' allowance adjustment and accommodate the construction inaccuracy in the field. A 12-ft lab prototype was built to test the solar energy harvest efficiency, the electrical energy storage, and the corresponding monitoring and data acquisition system. The lab test results demonstrated the constructability of the solar snow fence, the accuracy of the monitoring sensors, and the efficiency of the solar energy harvesting system. An average power of 829 Watts was generated daily for the 12-ft lab prototype. The fully verified solar snow fence system was then constructed with a helical piling method through a subcontractor. A 6-ft underground pile with an 8-ft above ground post constituted the frame of the solar snow fence. Pre-made connection holes on the posts provided smooth connections with the U brackets of the framed solar snow fence strips. The connection of the electrical wires with batteries and inverters was then followed. A modularized pattern was adopted in the solar panel connections so that the system would still be up and running when one of the solar panels broke. The construction of the solar snow fence was completed in 72 hours with additional monitoring and connection adjustment added on gradually.

Operation monitoring and data collection were followed after the field construction. A monitoring camera was installed on the first post of the solar snow fence to monitor the stability and safety of the whole solar snow fence. Temperature, moisture, solar intensity, wind speed, voltage, and current in the project were collected. An AT&T wireless plan was used to transmit the data collected through a Raspberry Pi. From the data collected, the solar snow fence generated about 11-25 kW*h per day, which can provide the power usage of a middle-size family. The drifted snow profile contained by the solar snow fence and the traditional snow fence were collected and compared. It was found the solar snow fence contained more drifted snow due to its low porosity (42%) and high stiffness.

The economic viability of the solar snow fence system varies across different scenarios. Solar snow fences with Power Purchase Agreement (PPA) contracts show promising financial returns with positive Net Present Values (NPVs) and high Internal Rates of Return (IRRs), indicating potential profitability. The scalability of the project is a critical factor. Larger projects, such as those covering 1 mile, could benefit from economies of scale, potentially reducing costs and enhancing their overall economic performance.

Improvement of the system connection between the photovoltaic (PV) panel and the steel post design is critical for cost-effective purposes. Currently, due to the high level of customization of the system, the cost of Module and BOS equipment remains higher than those of the cases using the National Renewable Energy Laboratory (NREL)-referenced estimations. However, longer span solar strips and less posts will largely reduce the cost of such a solar snow fence system.

With the data collected in this project, a field implementation of solar snow fence has been completed. The data collected shows that sizeable energy could be generated through the system. Wider implementation becomes cost effective when longer span solar strips and fewer posts are adopted.

Chapter 1: Manufacturing solar snow fence strips

1.1 Solar strip and its connection design

Based on the designed capacity (5 kW) of the solar system, 6'x6''x1/8'' solar strips were selected, with a designed capacity of 40w for each strip. Due to the fragile behavior of the solar strips, the solar strip is framed into a T-slotted aluminum frame (Figure 1.1) and a sliding bracket (Figure 1.2) is connected to the frame through sliding rivets at the two ends of the T-slotted frame. Such a connection could allow the adjustments of the construction inaccuracy of steel posts. On the sliding bracket, there are two premade connection holes used to fasten the connection brackets of the assembled solar strips with the steel posts.

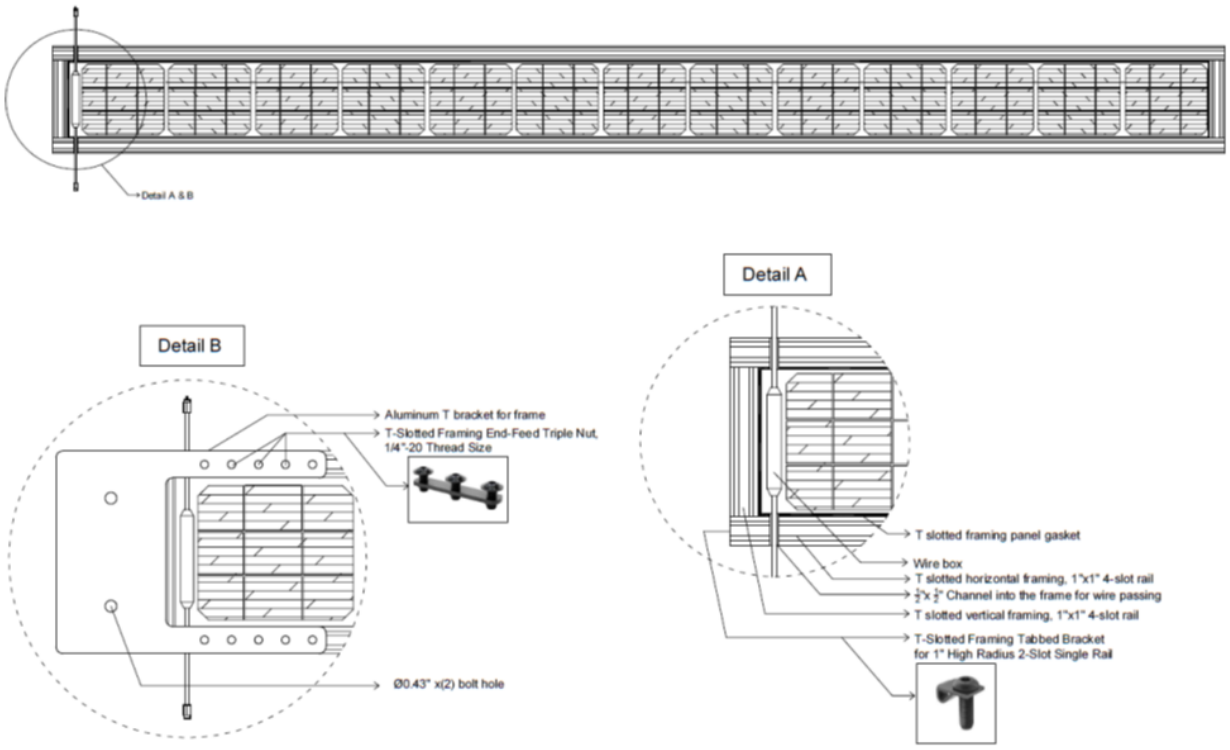

Figure 1.1 T-slotted solar strip frame

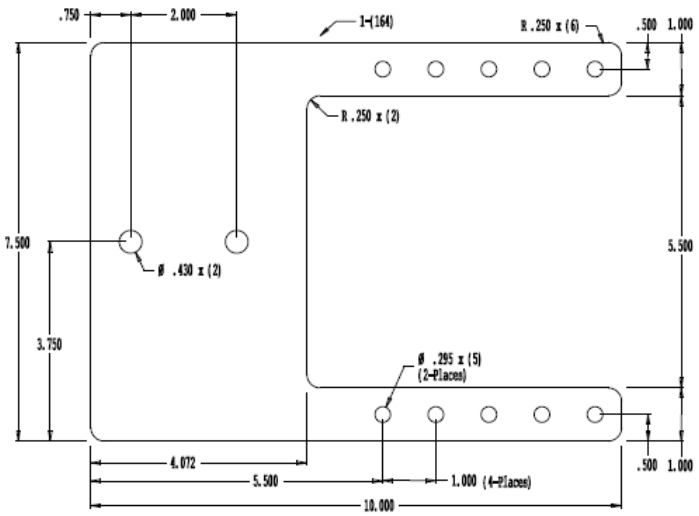

Figure 1.2 The connection bracket for the framed solar strips

1.2 Solar strip manufacturing and its fatigue testing

Figure 1.3 shows the framed solar snow fence strip manufactured in the lab. Due to the fragile behavior of the thermal glass used, the aluminum frame is used to protect the solar strip as shown in Figure 1.3. The solar strip is fixed to a 2x2-in. or a circular pipe (3.5x0.216) post through a U-bolt in the lab. The wind load is estimated to be 30 psf under 105 mph in Minnesota, considering the low elevation of the solar snow fence. Since,

$$P_Z = 0.00256K_ZK_dGV^2C_d \quad \text{(psf)} \tag{1.1}$$

Where P_Z is the wind load; the velocity pressure exposure coefficient $K_Z = 2.0\,(z/z_g)^{2/\alpha}$, z = 15 ft; K_d is the wind directionality factor; G is the gust effect factor, C_d is the drag coefficient, and V is the design wind speed. If the height of the solar snow fence above the ground is 16’ or less, z_g = 900, α = 9.5 and Table C3.8.4-1 in the AASHTO bridge design specification (BDS, 2018) gives K_Z = 0.85.

K_d = 0.85 (from AASHTO BDS Table 3.8.5-1)
G = 1.14 (from AASHTO BDS Table 3.8.6)
V = 105 mph
C_d = 1.26 for L/W = 12 (from AASHTO BDS Table 3.8.7-1)

$$P_Z = 0.00256 \times 0.85 \times 0.85 \times 1.14 \times 105^2 \times 1.26 = 29.3 \text{ psf} \tag{1.2}$$

The wind load is rounded to 30 psf for design convenience. For a 6’’x6’ strip, the resultant wind load is 90 lbs on each solar strip. For serviceability of 30 years, 10,000 cycle fatigue testing is conducted. A load of 100 lbs. is applied at the middle span of the solar strip through a 1-inch steel bar as shown in Figures 1.4 and 1.5. A load rate of 200 lbs. per minute is used to load the solar strip. Its displacement and the change of the solar strip and its connections are observed.

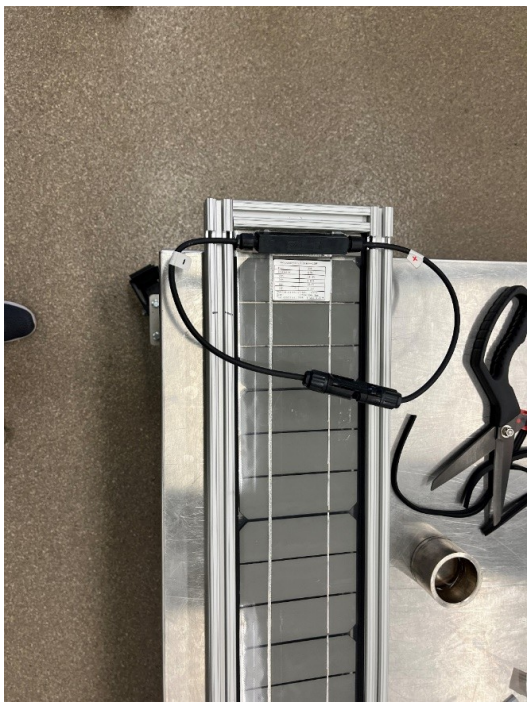

Figure 1.3 Assembled solar snow fence strip

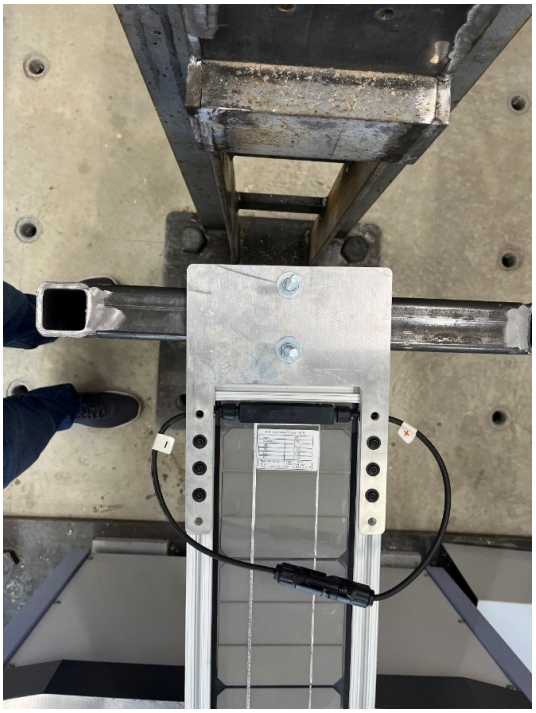

Figure 1.4 Front view of the fatigue test setup of the solar strip

Figure 1.5 Front view of the designed connection under fatigue testing of a 30 psf wind load

After 10,000 cycles of 100 lbs loading and unloading, the U-bolt connection is shown in Figure 1.6. From Figure 1.6, we can see the connection between the connection plate and the aluminum frame of the solar strip is intact and there is no degradation of the connection. We could also observe this from the load time history curve shown in Figure 1.7. The load time history is stable and can reach the full amplitude until the end of 10,000 cycles.

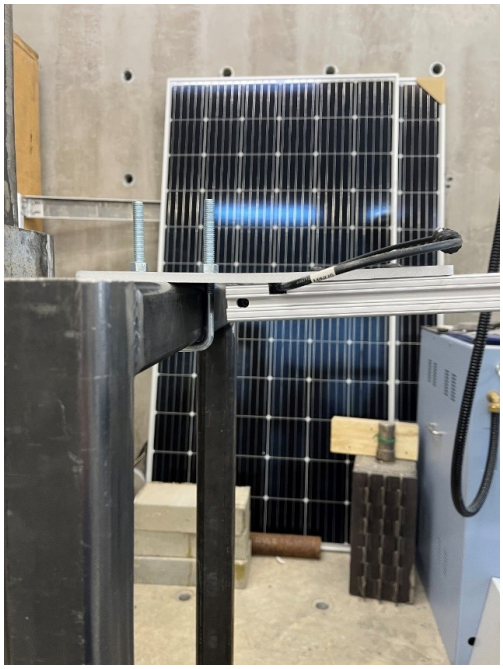

Figure 1.6 Front view of the designed connection under fatigue testing of a 30 psf wind load

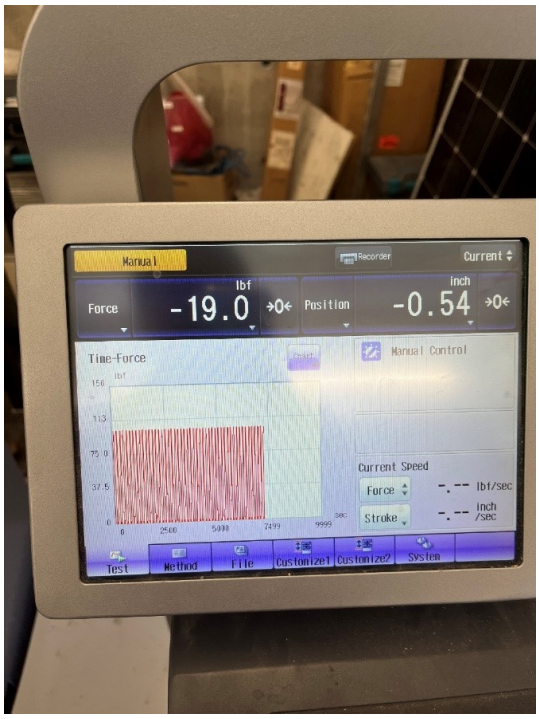

Figure 1.7 Load-time history of the fatigue test on the designed connection

Vertical setup is also used to check the possible sliding of the solar strip along the post under wind as shown in Figures. 1.8-1.11. A displacement control is used for the vertical test setup. A cyclic test pushes up the solar strip 1 in. in the middle and unloads it to 0.5 in. in 30 sec to mimic a 2 Hz shake. Ten thousand cycles are used. The final load time history and its load-displacement hysteresis is shown in Figures. 1.12-1.13.

Figure 1.8 Front view of the vertical direction test setup

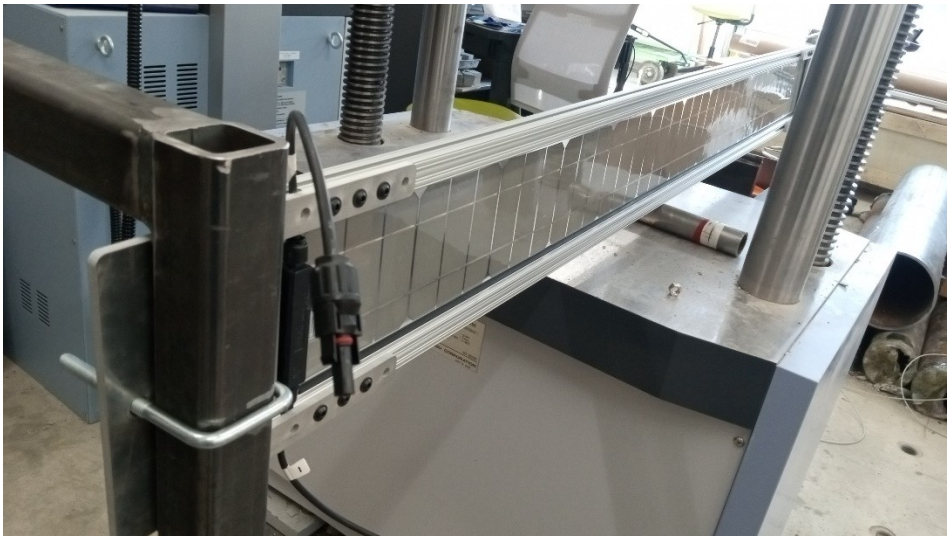

Figure 1.9 Back view of the vertical direction test setup

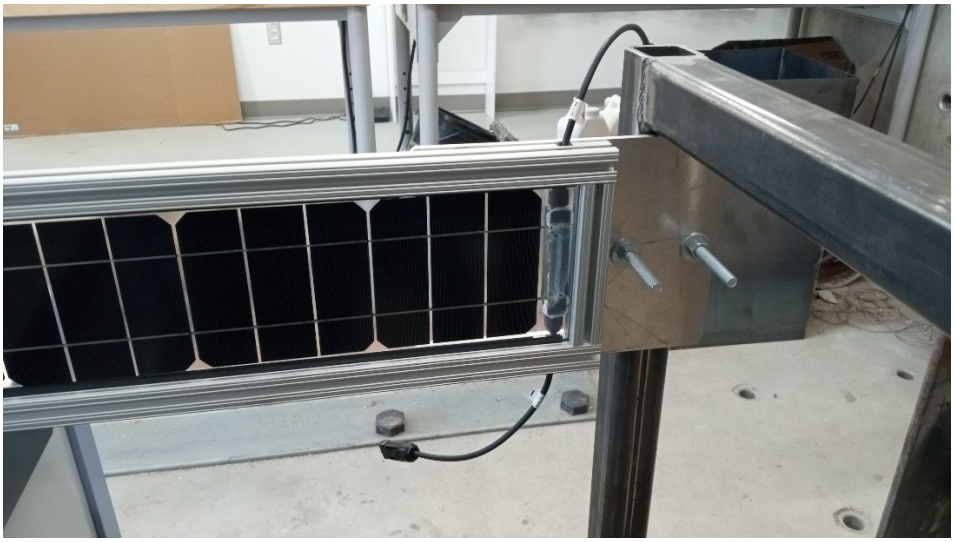

Figure 1.10 Zoom-in front view of the U-bolt connection in the vertical direction test setup

Figure 1.11 Zoom-in back view of the U-bolt connection in the vertical direction test setup

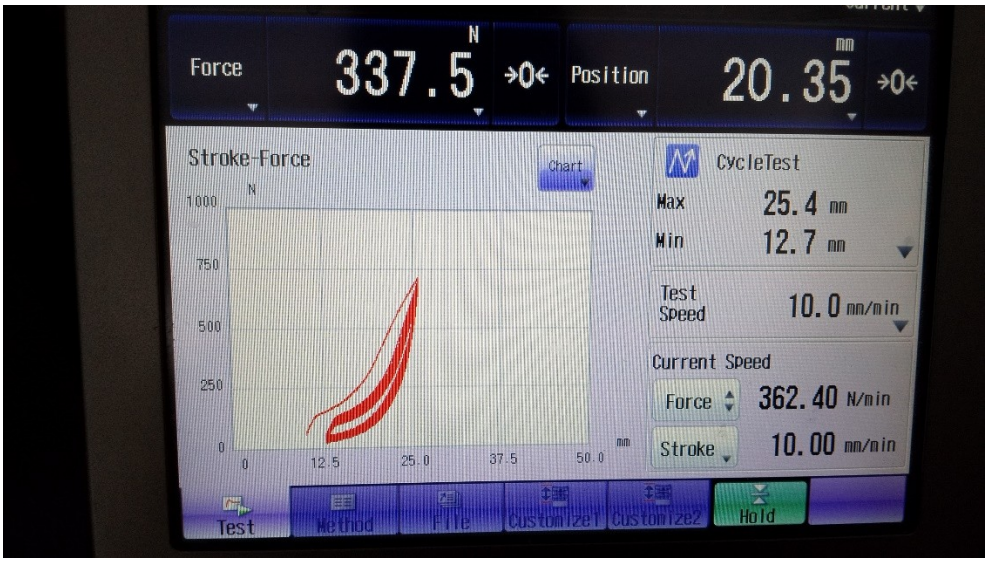

Figure 1.12 The load-displacement hysteresis of the vertical direction fatigue test results

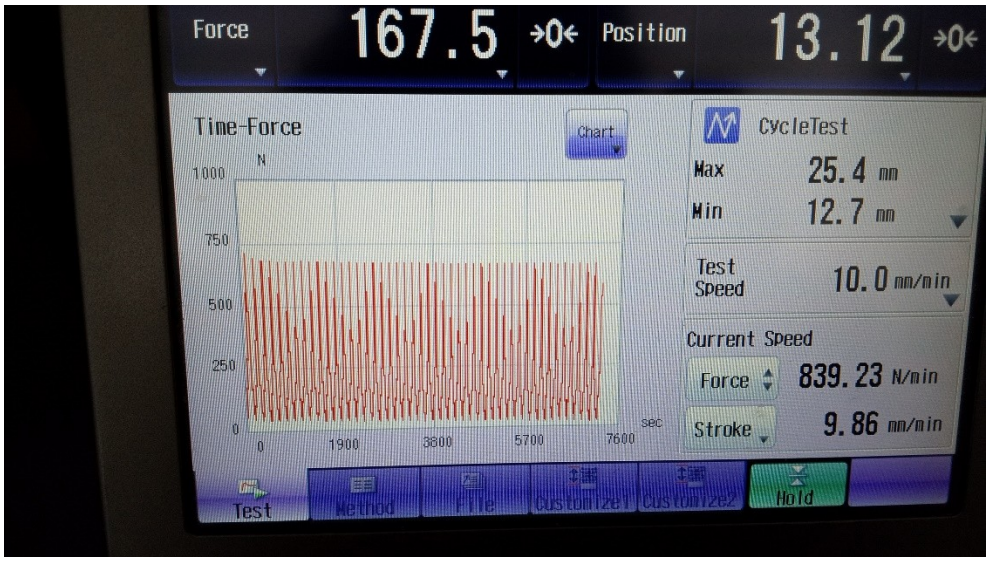

Figure 1.13 The load-time history of the vertical direction fatigue test results

From the test results in Figures. 1.12-1.13, we can see the solar strip and its connection design work well in the vertical direction as well. With 10,000 cycles of loading, there is no sliding or movement with a 1-inch pushup. The hysteresis loop and the load time story are stable and don't drift with time.

Chapter 2: Design, development, assembling, debugging, and packaging solar controllers and inverters under ambient working temperature conditions utilizing the environmental chamber available at NDSU

2.1 Design of the solar controller and inverter for the solar snow fence system

The solar strips are connected through wires in series for every 2 pieces between posts and in parallel with other groups. The output from each group contributes 40V and 2A output. Every eight subgroups are combined to output 80V and 16A through the charger and inverter (Figure 2.1), which prepares the output to be ready for usage or grid integration.

Connection:

Each panel: 40W/20V, i.e., 20V,2A

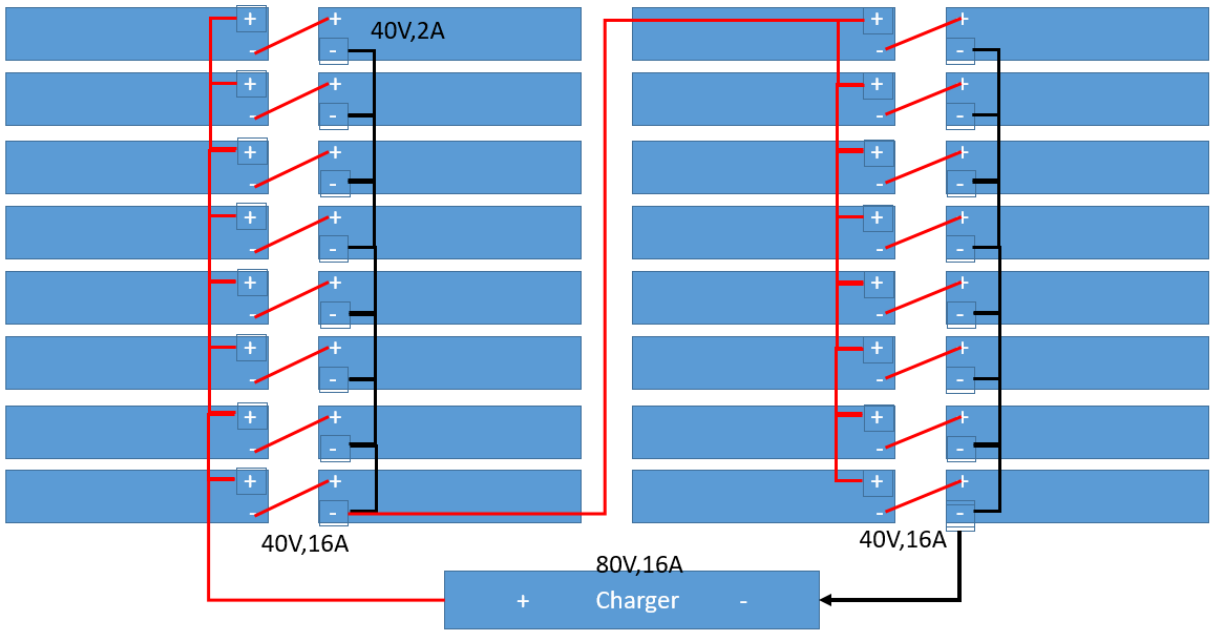

Figure 2.1 Connection diagram for solar strips

The overall solar snow fence system is shown in Figure 2.2. The power system (Figure 2.3) consists of a DC voltage source/solar panels, Charger, Batteries, and an Inverter (DC 24V to AC 110V).

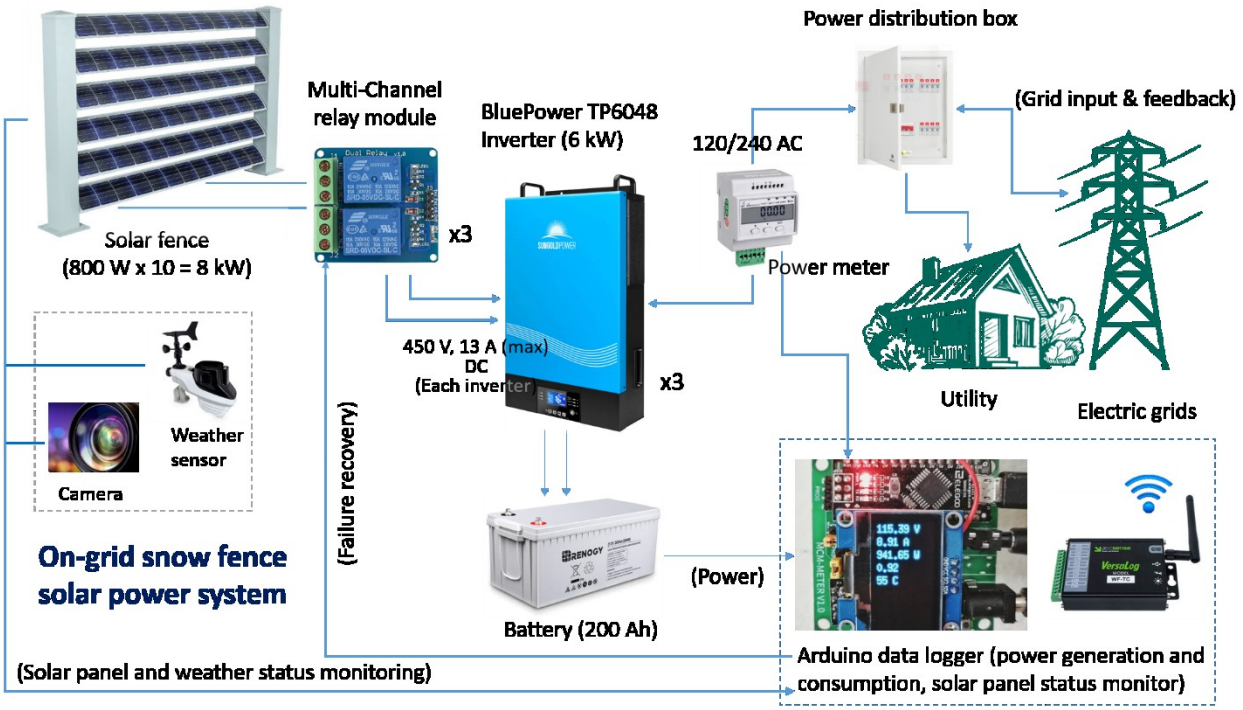

Figure 2.2 Overview of the whole solar snow fence system

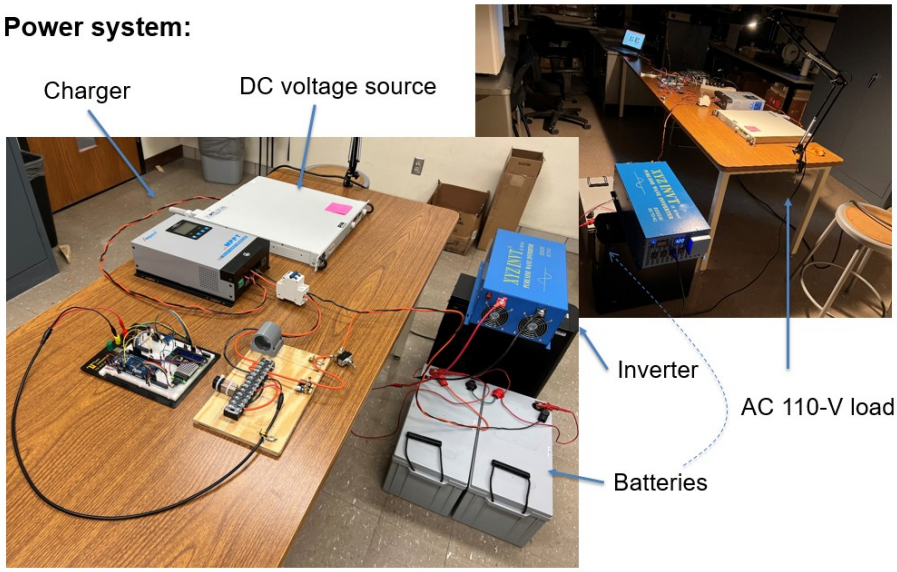

Figure 2.3 Power system converting 24-V DC electricity to 110-V, 60Hz AC electricity.

Light intensity, moisture, temperature, and output voltage and current sensors are installed in the monitoring system that works with the controller simultaneously (Figures. 2.4 and 2.5). Lab tests prove the connected system works well and outputs the monitored variables accurately.

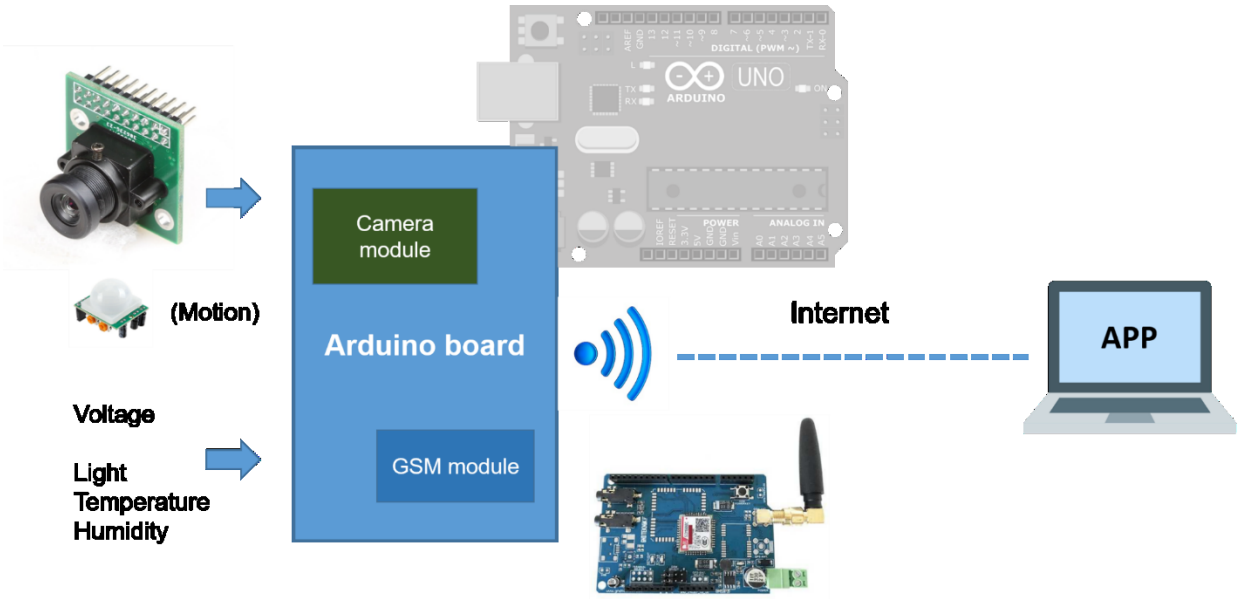

Figure 2.4 Overview of the monitoring module of the solar snow fence system

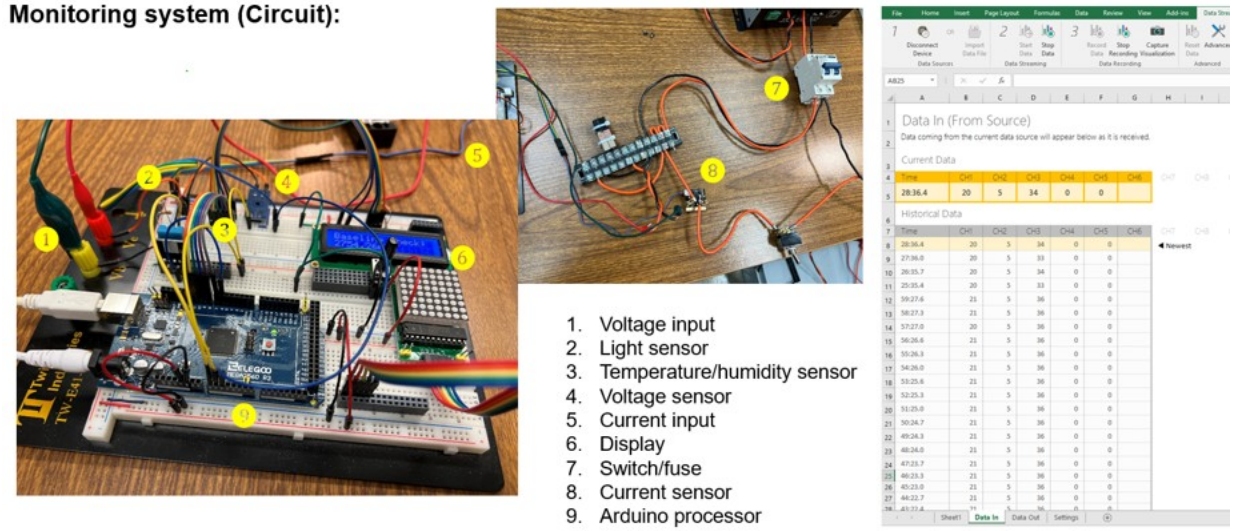

Figure 2.5 Circuit monitoring the environment parameters and solar panel status

A photo of the monitoring system is shown in Figure 2.5. The current system can detect the environmental parameters including Temperature, Humidity, Light intensity, and voltage and current, which are used to calculate the power generated by the solar panel system and the wind parameters for snow drifting. The data of the power system collected with the monitoring system are sent to a computer, where the parameters of Temperature, Humidity, Light Intensity, Voltage, and Current recorded each minute are shown and saved in an Excel file.

2.2 Lab prototype of the solar snow fence system

A prototype system based on the design in Task 2.1 was constructed in the lab, which is shown in Figures 2.6-2.9. The solar strip manufacturing, the connection between the solar strip frames with the steel posts, and the designed power and monitoring systems are tested and functioned well.

Figure 2.6 Front side of the prototype solar snow fence constructed in the Lab.

Figure 2.7 Back side of the prototype solar snow fence constructed in the Lab.

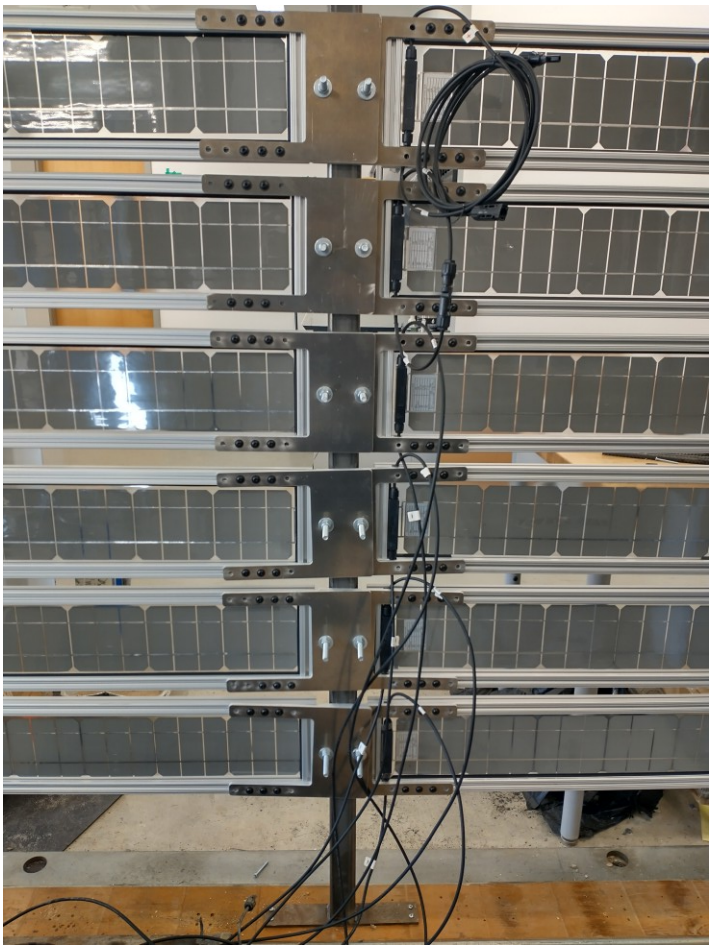

Figure 2.8 The back side U bolt connection adopted for the solar snow fence system.

Figure 2.9 The front side of the U bolt connection adopted for the solar snow fence system.

2.3 Lab prototype of the solar snow fence system and its testing

Systematic testing has been performed to validate the solar snow fence system and the sensors used and check its energy generation performance. Validation of sensors was first conducted. A validation of the moisture sensor and the temperature sensor are shown in Figures 2.10-2.13. The validation of moisture sensor was conducted in the Environmental chamber at North Dakota State University (NDSU) Ehly 110 Advanced Structural Lab. 30% and 95% of moisture level were set in the Environmental Chamber. And the sensor monitored moistures are shown in Figure 2.11. The monitored data showed relatively good accuracy in the low moisture level but excellent accuracy when the moisture level is high. Temperature sensors were also validated in the lab through a temperature oven in the same lab (Figure 2.12). A preselected 30^{o}C is chosen and the monitored temperature is shown in Figure 2.13. The data showed excellent accuracy of the temperature sensor selected. The addition of bypass diodes, field monitoring via a camera, and sending data wirelessly via the internet in order to monitor and control the solar snow fence system remotely has been completed and integrated to the solar snow fence prototype shown in Figure 2.14. And the power generated through the solar snow fence prototype on May 25th, 2023, is shown in Figures 2.15-2.16. An average of 160w electricity is generated during the

day. Please note the prototype only uses 6 strips for each span, but it will be 8 strips for the field implementation.

Figure 2.10 Testing of the solar snow fence system for its moisture sensor in the NDSU environment chamber.

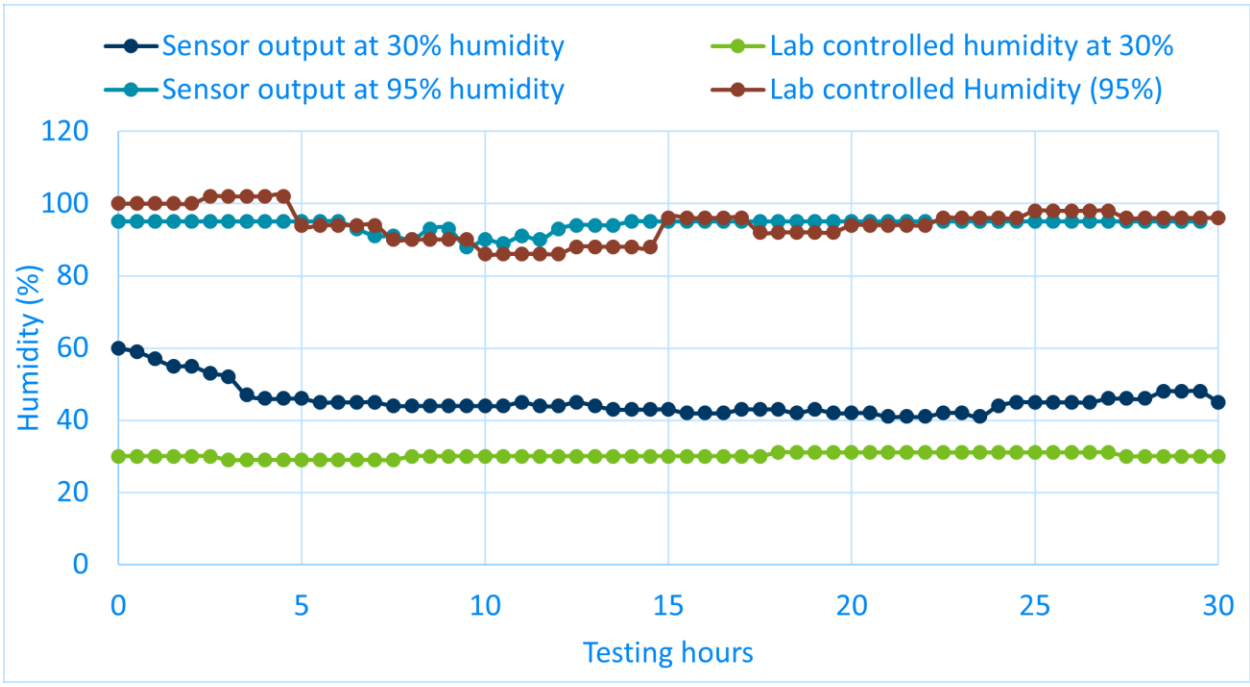

Figure 2.11 The preset and monitored moisture level in the NDSU environment chamber through the moisture sensor of the solar snow fence monitoring system.

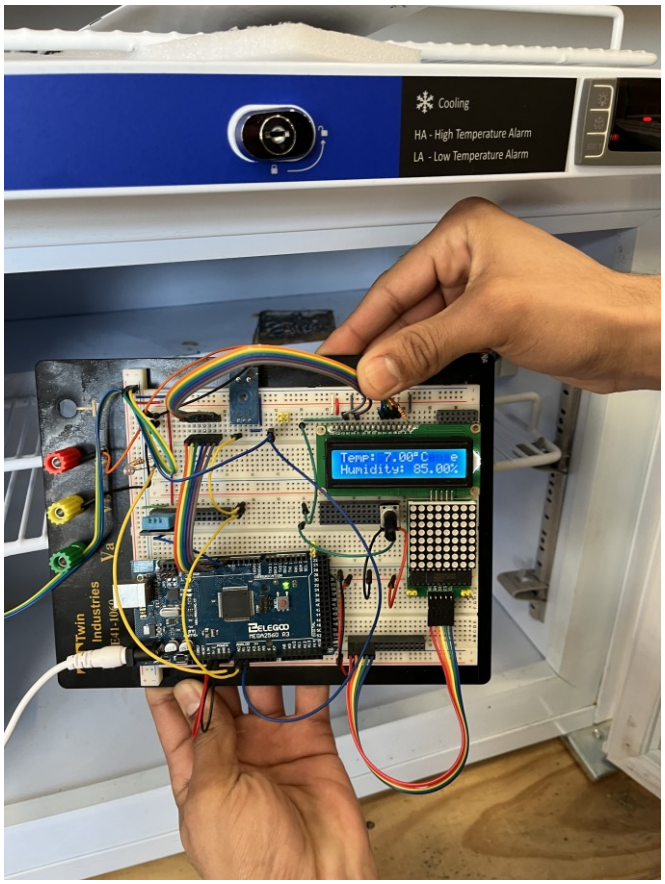

Figure 2.12 Testing of the solar snow fence system for its temperature sensor in the NDSU environment chamber.

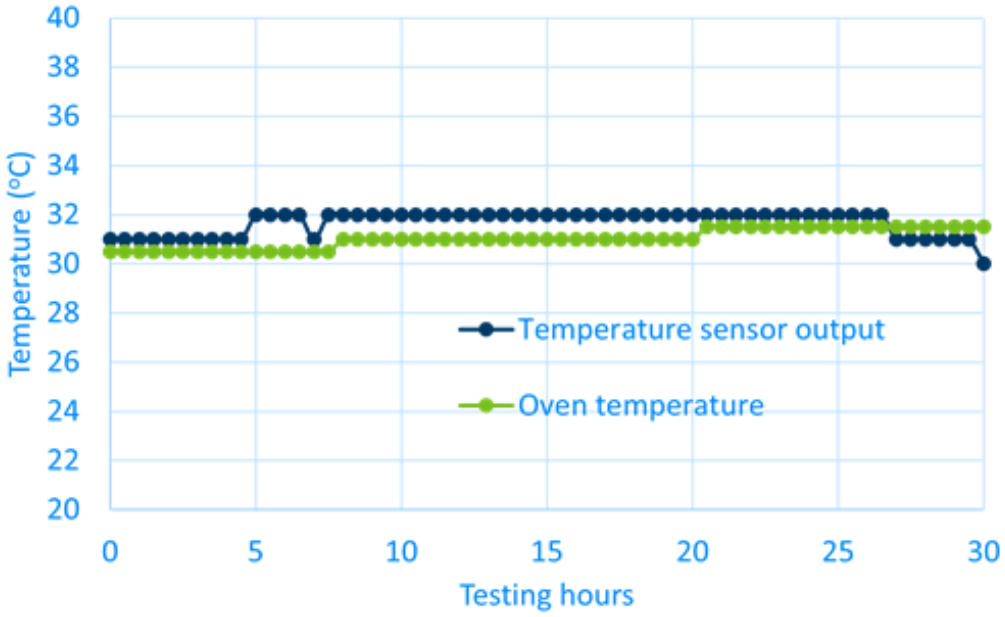

Figure 2.13 The preset and monitored temperature in the NDSU environment chamber through the temperature sensor of the solar snow fence monitoring system.

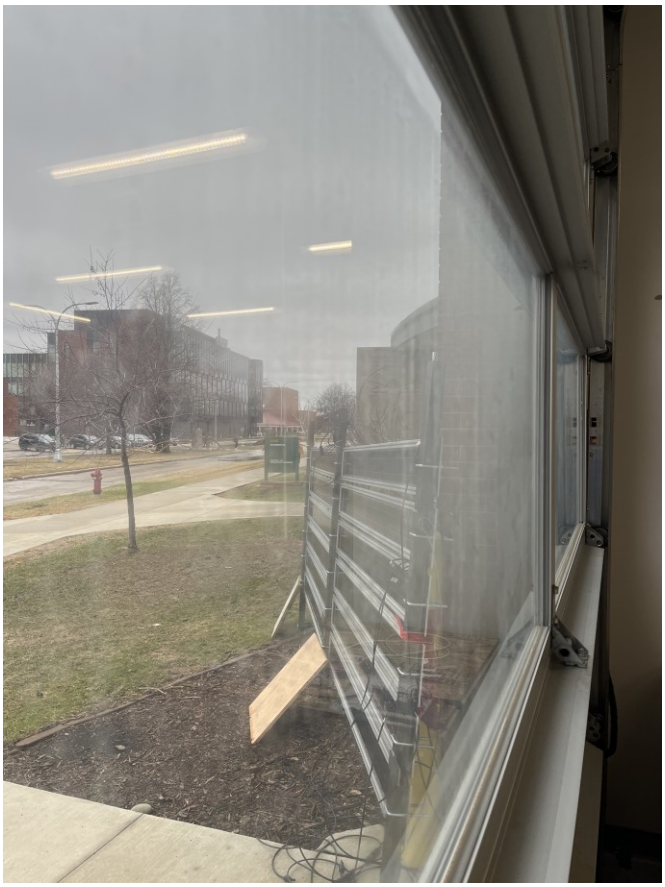

Figure 2.14 Testing of the solar snow fence system for its energy generation in the NDSU Ehly 110 Advanced Structural Lab.

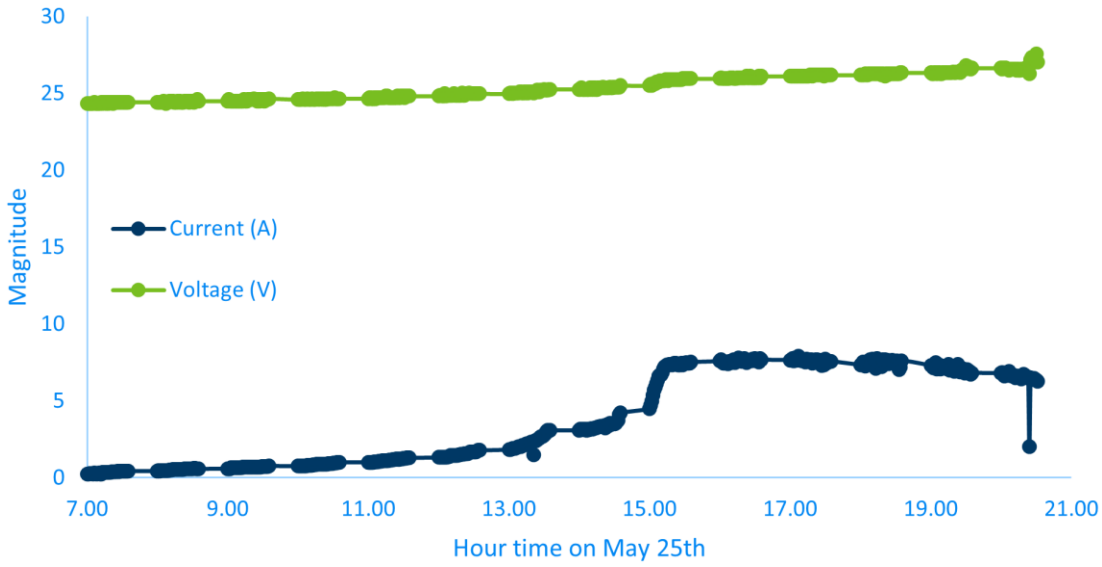

Figure 2.15 Time current and voltage history generated on May 25th 2023.

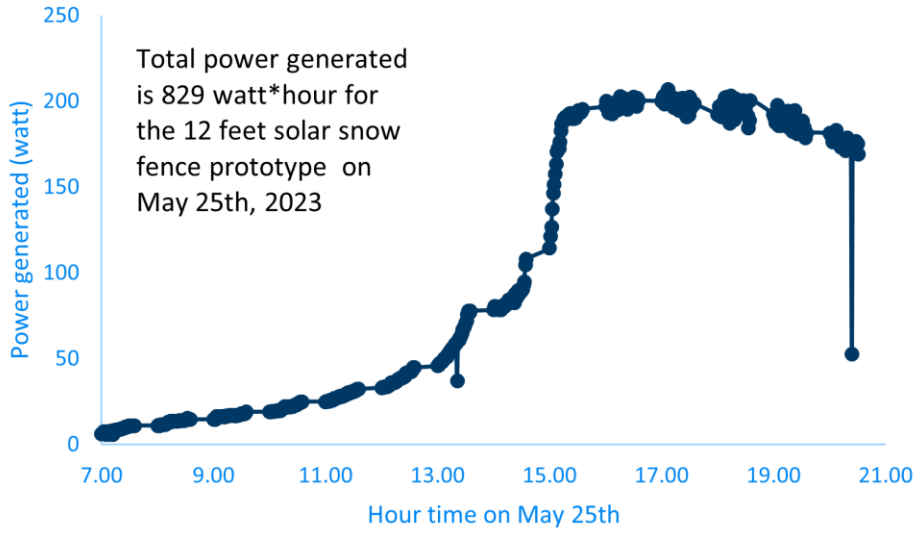

Figure 2.16 Power generated on May 25th, 2023 at the 12 feet solar snow fence prototype.

Chapter 3: Lab verification, field construction, and testing of the solar snow fence system

3.1 Site survey

A site survey was conducted on Sep 15th, 2022 to determine the location for the installation of the solar snow fence and plan out the integration of the solar snow fence system with the existing snow fence, sensor placement, construction logistics, and off-grid electrical power use. A site was finally selected as shown in Figure 3.1. MnDOT proposed to install the 100-ft solar snow fence at the east end of the existing snow fence and compare it with the original snow fence on their performances.

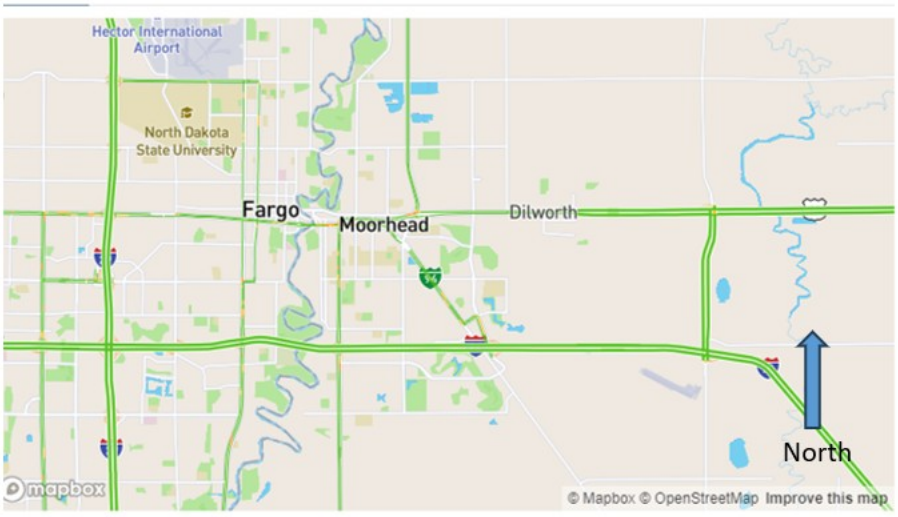

(a) Orientation of the site location

(b) The location of the project site

Figure 3.1 Map of proposed solar snow fence location.

The site is characterized as nearly level, with the ground consisting of clay with widespread native vegetation approximately 1 to 36 inches in height. The prototype solar snow fence will be offset by 2 ft from the existing 8-foot plastic snow fence.

Geotechnical work for use in the design and engineering of the solar snow fence foundation has been checked. The project began with a field construction through TechnoMetalPost, Inc., followed by the installation of solar strips and debugging of the electric system and the monitoring units including camera monitoring and remote data collection.

3.2 The electrical solar fence system implemented in the field and its working circuit

Due to the protection aluminum frame adopted in the solar strips for the solar snow fence system, the porosity of the snow fence system changed from 50% to 42%, and the bottom gap was increased from 6'' to 17'', considering the bottom strip will not be able to capture the sun lights during winter times. The solar strips were connected through wires in series for every 2 pieces between posts and in parallel with other groups. The output from each group contributed 40V and 2A output. Every two subgroups were combined to output 80V and 14A to the charger (Figure 3.2) and passed to the inverter, which will prepare the output to be ready for usage or grid integration.

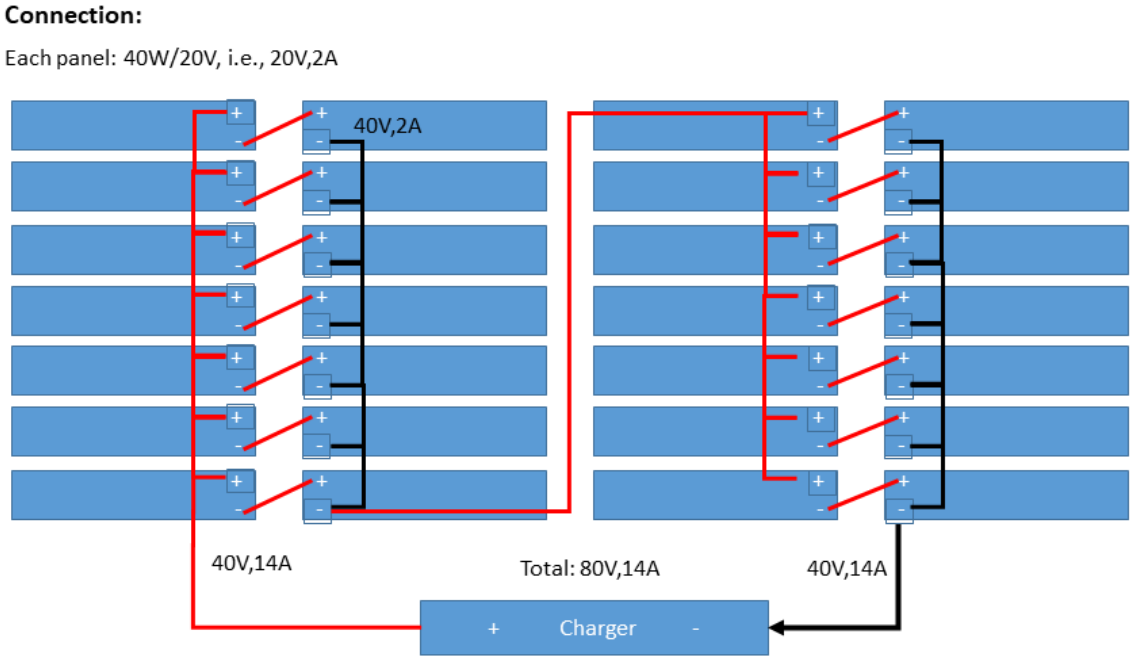

Figure 3.2 Connection diagram for solar strips.

As to the connections between units in the developed power system, four modules are independent with respect to each other. This configuration will be able to avoid system failure when one piece is broken (Figure 3.3).

The controller and its monitoring system have been designed and tested in Lab and implemented in field. At the same time, a monitoring camera is set in the field that monitors the project site through an AT&T wireless data plan.

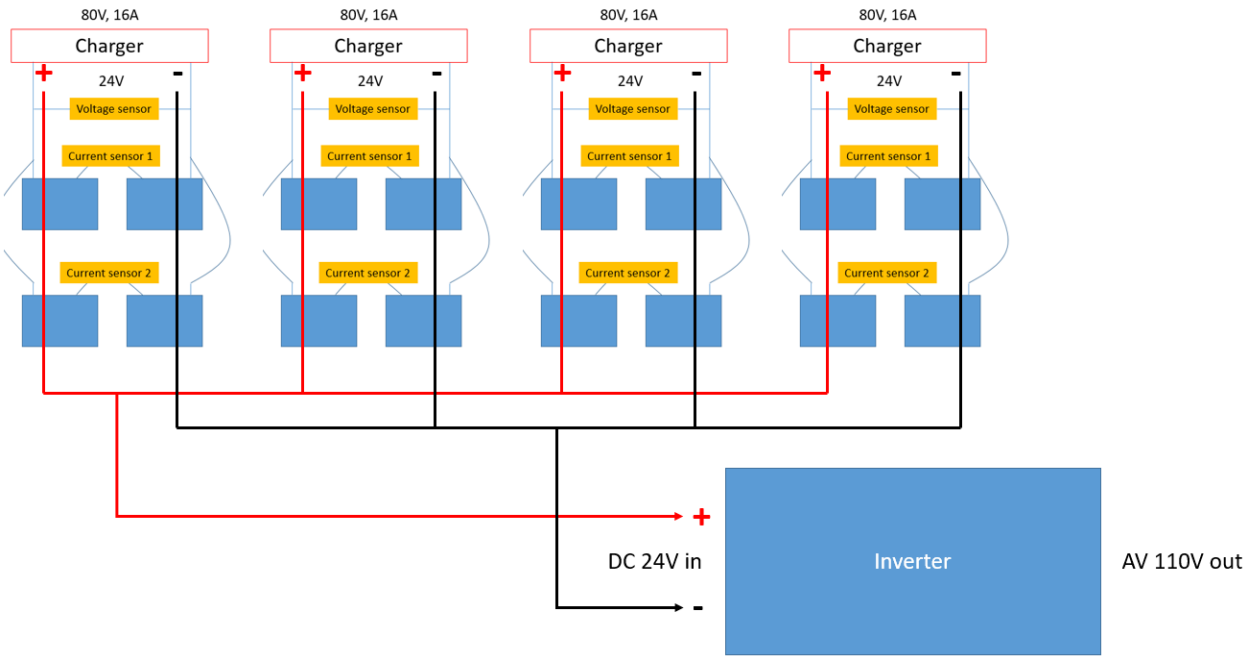

Figure 3.3 The battery connection system.

3.3 Field construction and testing of the solar snow fence system

The prototype solar snow fence was placed 2 ft in the front of the existing 8-foot plastic snow fence and has a 2 ft overlap with the original snow fence. A total of seventeen metal helical posts 3.5 inches in diameter have been completed to support the solar snow fence. Four additional 3.5 inches metal helical piers were also constructed to support the electrical equipment and sensors cabinet, as shown in Figures 3.4-3.5.

(a) View of completed posts in E-W direction

(b) View of completed posts in S-N direction

(c) Post construction in progress.

(d) Welded connection to connect helical pile with the above ground post

Figure 3.4 Helical pier drilling and solar snow fence post construction.

(a) Connection of solar panels onto posts (b) View of strips of solar snow fence

Figure 3.5 Connected solar strips on posts.

3.4 Field camera monitoring and data collection

3.4.1 Camera selection and installation

Reolink camera RLC-410W was selected for field monitoring. The camera was installed through a wood frame stuck out from the first post (Figure 3.6). The camera was linked to an Alcatel router and wifi connected through an AT&T wireless plan.

Figure 3.6 Installed camera.

After linking the IP address of the camera with the router, the camera can lively stream the field conditions to the Reolink app installed on any mobile phone or computer. A live picture from the camera is shown in Figure 3.7.

Figure 3.7 A live photo from the camera installed in the project site.

3.4.2 Solar snow fence monitoring and data collection system

Arduino and PI system were used to monitor the field and collect the data in field remotely. The mechanism of the monitoring system is shown in Figure 2.5. The wind speed, solar intensity, temperature, moisture, voltage, and current sensors are adopted and shown in Figure 3.8.

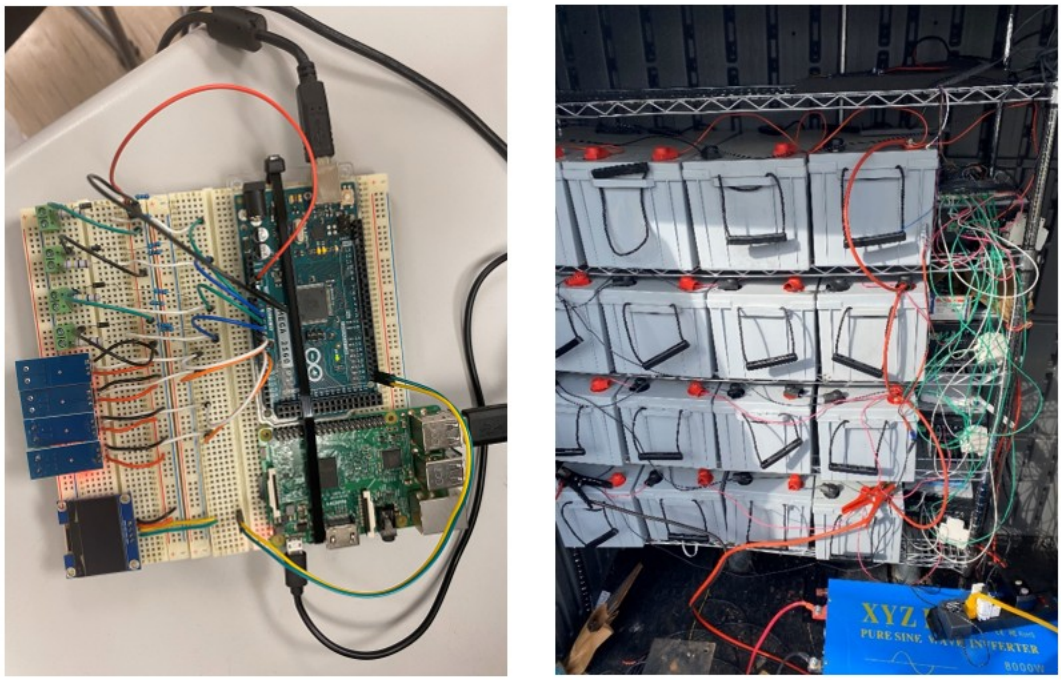

(a) Data acquisition board (b) Battery system adopted

Figure 3.8 The solar snow fence monitoring and data collection system.

The Arduino module collected all the sensor data and transmitted the data through the Pi module. A remote server could be set up on any computer to collect the data as shown in Figure 3.9.

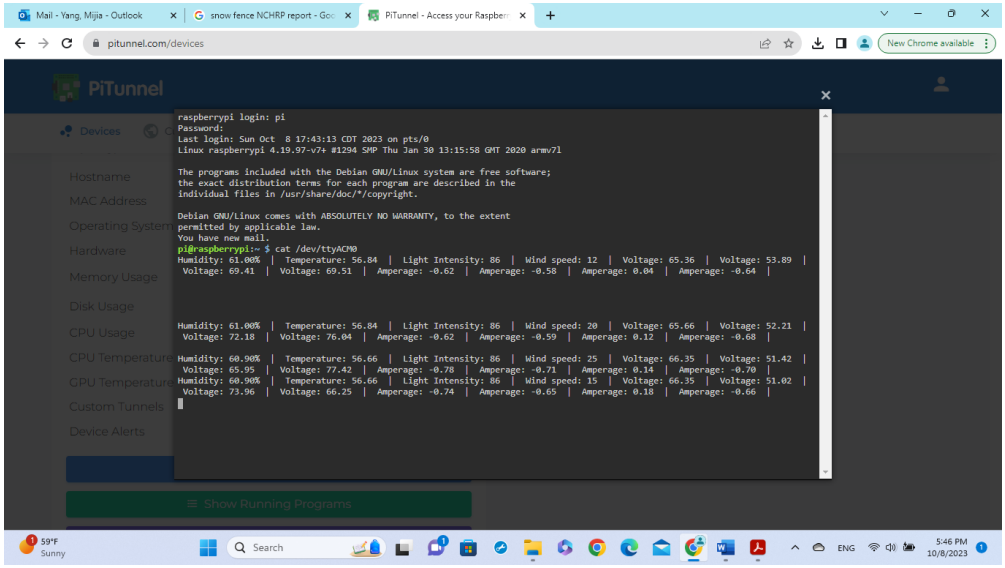

Figure 3.9 Screen shot of the remote server for the solar snow fence monitoring and data collection system.

3.4.3 Usage of the solar energy in snow melting and monitoring system powering

The energy produced through the solar snow fence is used to power 3 snow melting pads. Each snow melting pad consumes power at 450W. The camera and the solar snow fence monitoring data collection system consume 450W as well. The total power consumption is estimated at 1.8 Kw, while the output power of the solar snow fence system is calculated at 3.84 Kw and the input power from the solar strips is at 4.48 Kw.

The field photo of the system is shown in Figure 3.10, where three snow-melting pads are shown in the photo.

Figure 3.10 Snow melting pads powered by the solar snow fence system.

Three heattrak snow-melting pads are purchased and adopted to melt the snow around the control room and the west end of the solar snow fence. The heattrak could be remotely controlled through a smart home app (Figure 3.11). The heattrak pad consumes 450 Watts*hour every hour. Each pad works for 5 hours every day and is arranged for 5.0 hours in turn. Based on the snow-melting capacity of the heattrak pad, it can melt 2'' per hour and melt 10'' in 5 hours. Maximum snow precipitation is 10 inches on average in Fargo, ND from October to April, which can be effectively handled by the heattrak snow melting pads.

Figure 3.11 Snow melting pads controlled remotely by the smart home app.

3.5 Performance of the solar snow fence system

The solar snow performance data was collected on Nov 19th, 2023. The data is shown in Figures 3.12-3.14. The voltage from the solar snow fence can reach the designed 80 volts most of the daytime, as shown in Figure 3.12. One of the voltage sensors is saturated due to the base voltage offset. Small variations are caused by the clouds in the sky. The current from the solar snow fence circuit is also recorded, which is around 0 to 12 Amps most of the time. On Nov 19th, 2023, the current is recorded at around 6 Amps in the daytime from 8:00 AM-4:00 PM (Figure 3.13), which is mainly due to the fact that the battery is 80% fully charged and the usage of the power produced is small. The current varies in the circuit. When the battery is empty, the charging process works with the highest efficiency and the current is the highest. When the battery is full, the charging process is close to a stop and the current is the smallest. Payload comes into the picture as well and it balances out the energy produced through the solar strips and increases the current in the circuit. Based on the current and voltage recorded on Nov 19th, 2023, the power harnessed is shown in Figure 3.14, which indicates a 1.5 kW production on Nov 19th, 2023 during 8:00 AM to 4:00 PM from the three modules (one of the modules did not collect the voltage and current data correctly due to loose contact). The solar snow fence begins to produce energy when the sun rises, around 6 to 8 AM. It comes to an end when the sun sets around 8:00 PM. The stored energy is used for different purposes, such as wifi communication and snow melting.

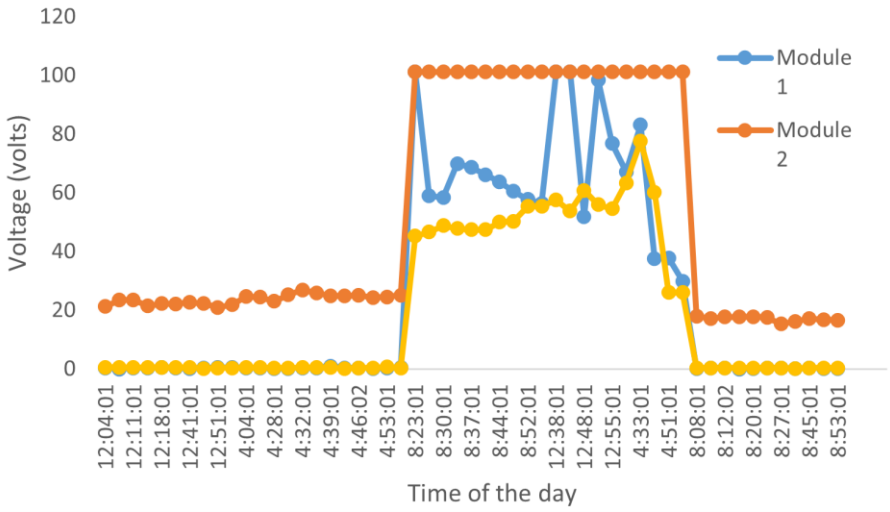

Figure 3.12 The voltage time history on Nov 19th, 2023.

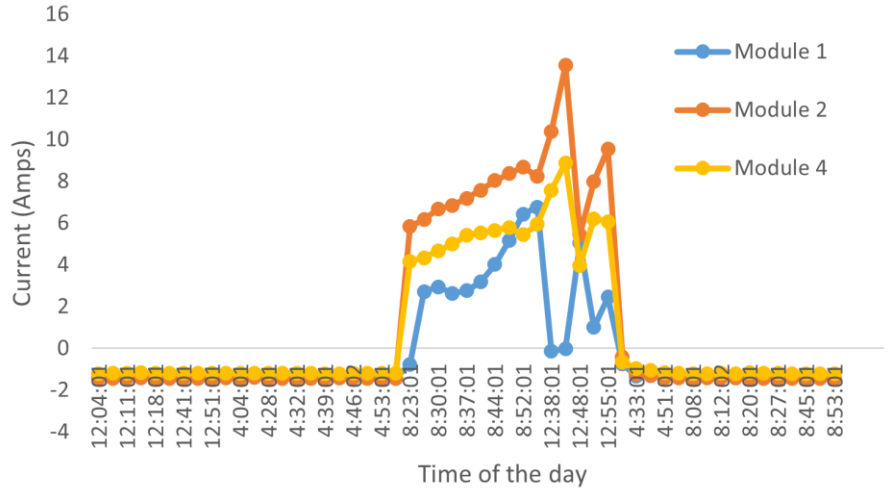

Figure 3.13 The current time history on Nov 19th, 2023.

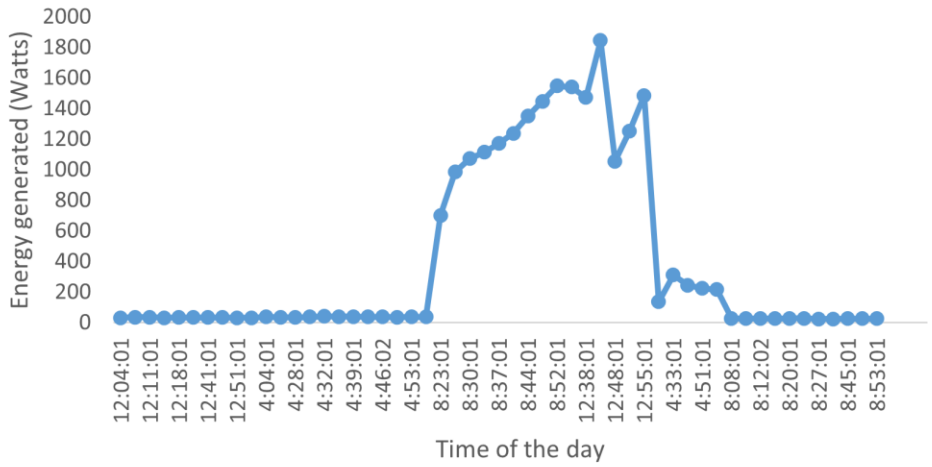

Figure 3.14 Power harnessed on Nov 19th, 2023.

At the same time, external environmental factors are collected as well, which includes humidity, temperature, solar intensity, and wind speed. The humidity time history is shown in Figure 3.15, which indicates an average of 50% humidity during the day from 8:00 AM to 12:00 PM. The temperature time history is shown in Figure 3.16, which is around 40°F. Solar intensity is observed to be around 85%, which indicates a sunny day with a few clouds during the day (Figure 3.17), with the full solar intensity at 1000 Watts/m^2. The wind speed on that day was around 16 mph (Figure 3.18).

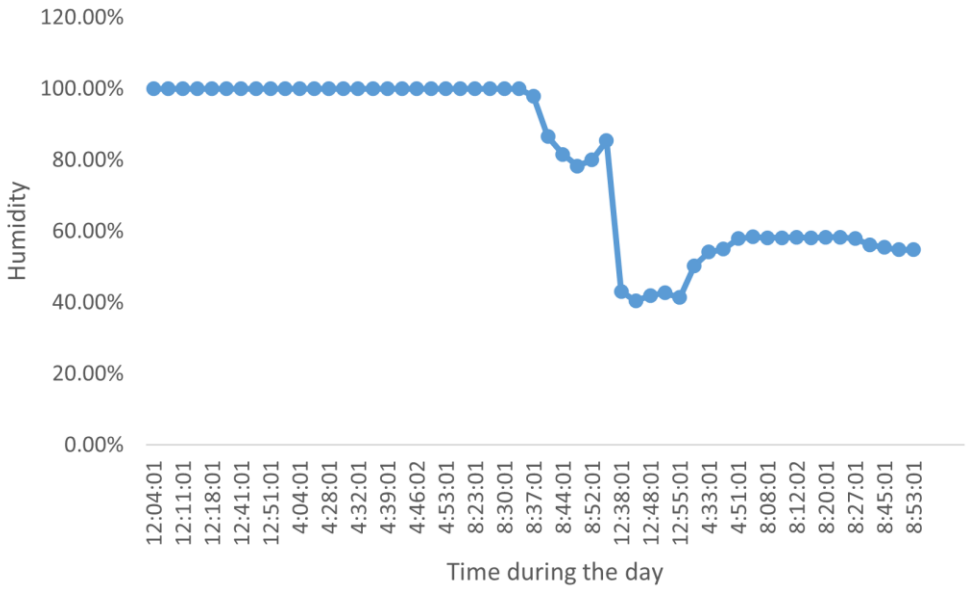

Figure 3.15 The humidity time history on Nov 19th, 2023.

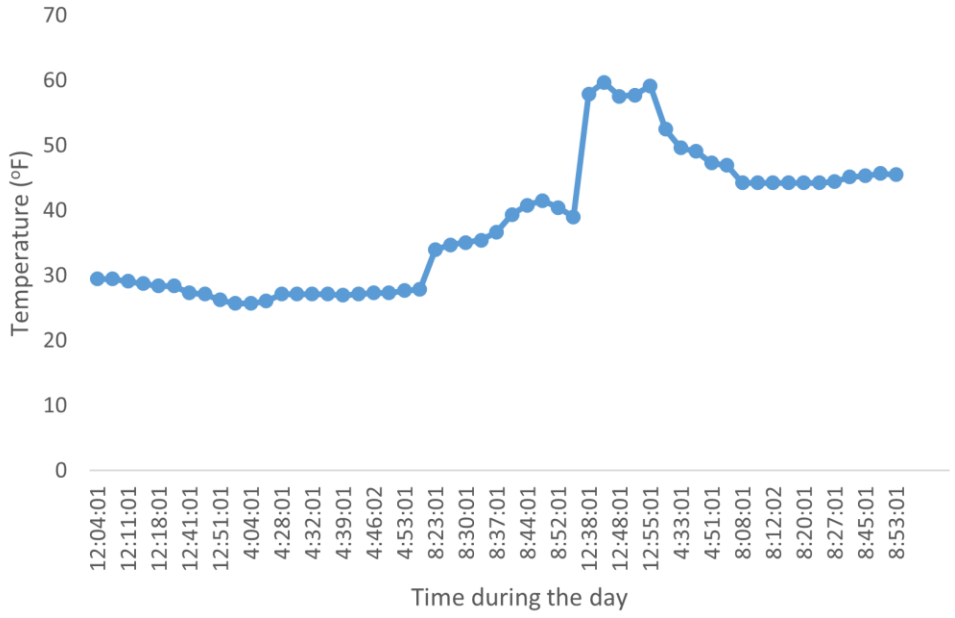

Figure 3.16 The temperature time history on Nov 19th, 2023.

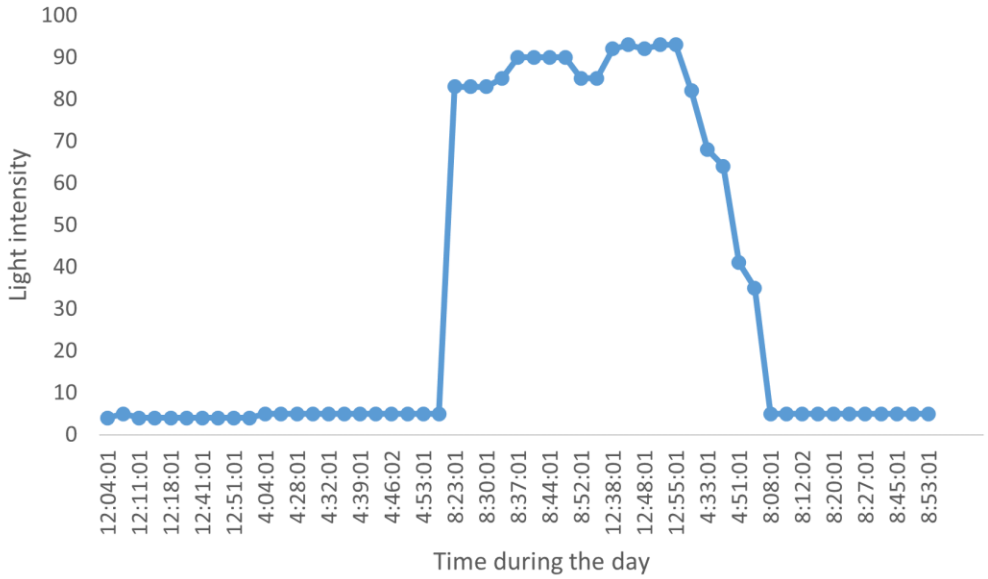

Figure 3.17 The solar intensity time history on Nov 19th, 2023.

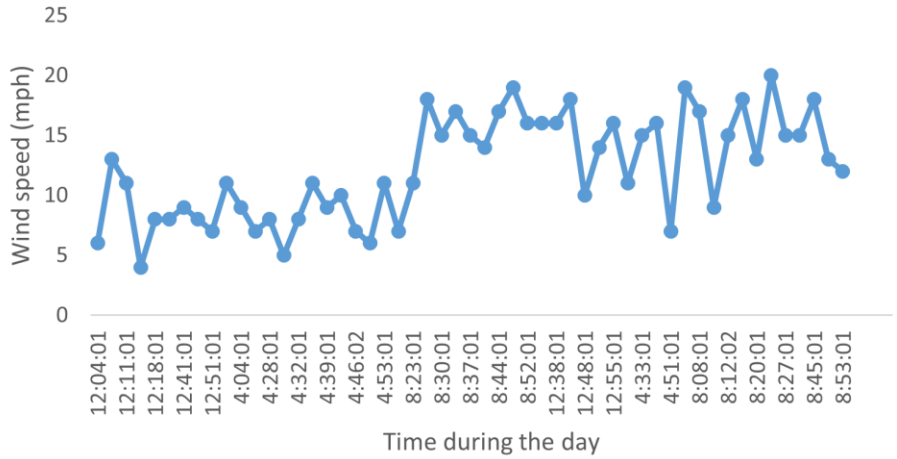

Figure 3.18 The wind speed time history on Nov 19th, 2023.

The data on Nov 18th, 2023 was also collected. The data is shown in Figures 3.19-3.25. The humidity time history on Nov 18th is shown in Figure 3.19. An average of 60% humidity is observed, which is consistent with the weather underground data (https://www.wunderground.com/history/daily/us/nd/fargo/KFAR/date/2023-11-18). The temperature time history is shown in Figure 3.20, which is around 40°F and consistent with the weather underground data as well. The light intensity data and the wind speed data are shown in Figure 3.21 and Figure 3.22. The voltage from the solar snow fence can reach the designed 80 volts most of the time, as shown in Figure 3.23. Small variations are caused by the clouds in the sky. The current from the solar snow fence circuit is also recorded, which is around 0 to 12 Amps most of the time. On Nov 18th, 2023, the current is recorded at around 10 Amps in the daytime (Figure 3.24). The power of the solar snow fence on Nov 18th, 2023, is shown in Figure 3.25, which reaches 1.2 kW from the three modules and is a bit far away from the design power (4.48 kW) due to the fair weather condition in a typical late Fall day.

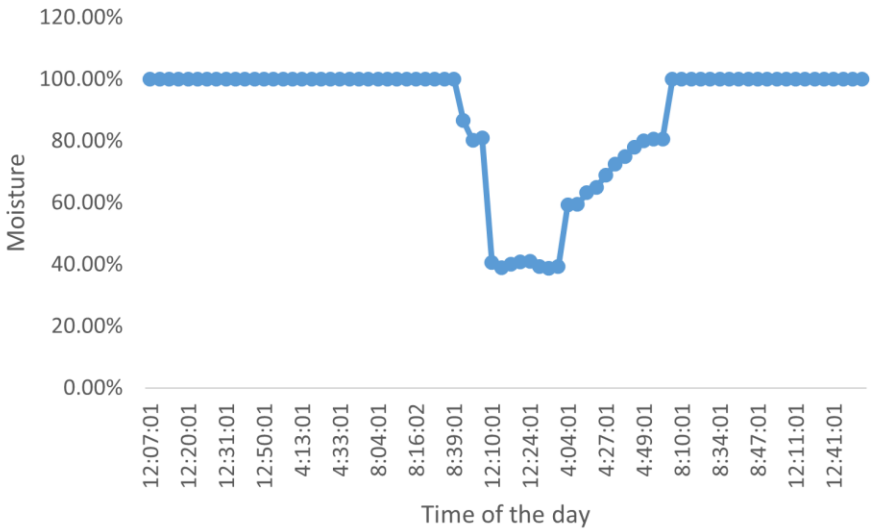

Figure 3.19 Humidity time history on Nov 18th, 2023.

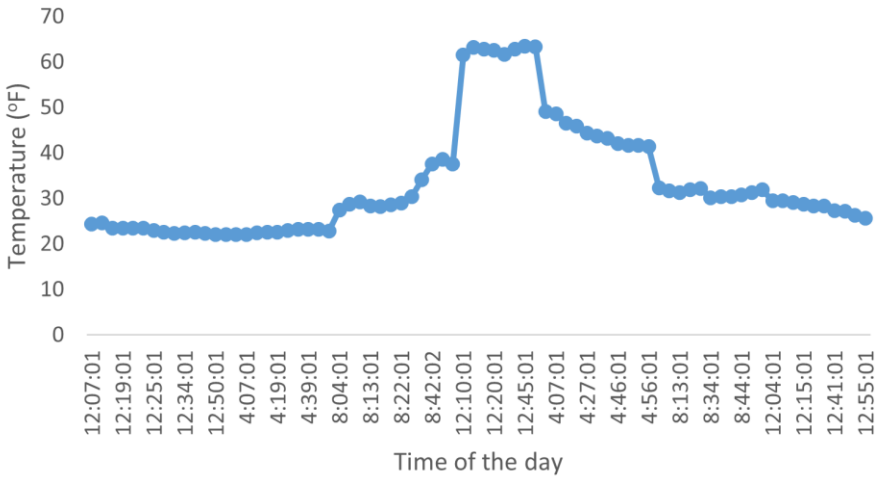

Figure 3.20 Temperature time history on Nov 18th, 2023.

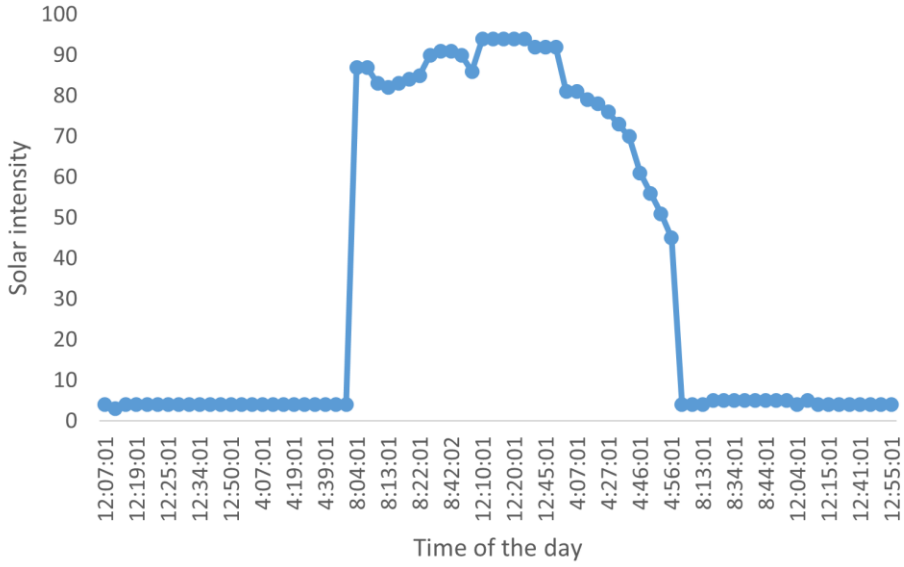

Figure 3.21 Light intensity time history on Nov 18th, 2023.

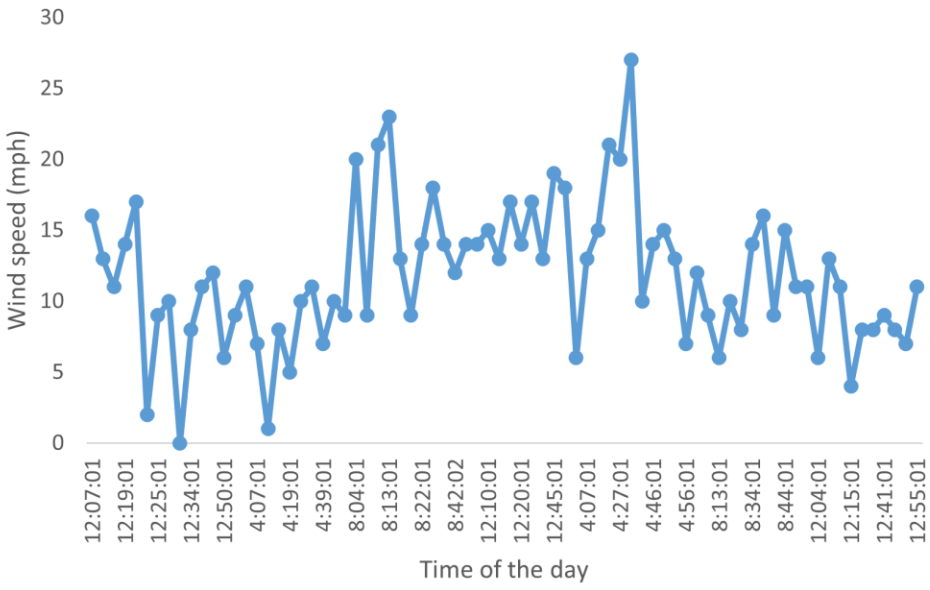

Figure 3.22 Wind speed time history on Nov 18th, 2023.

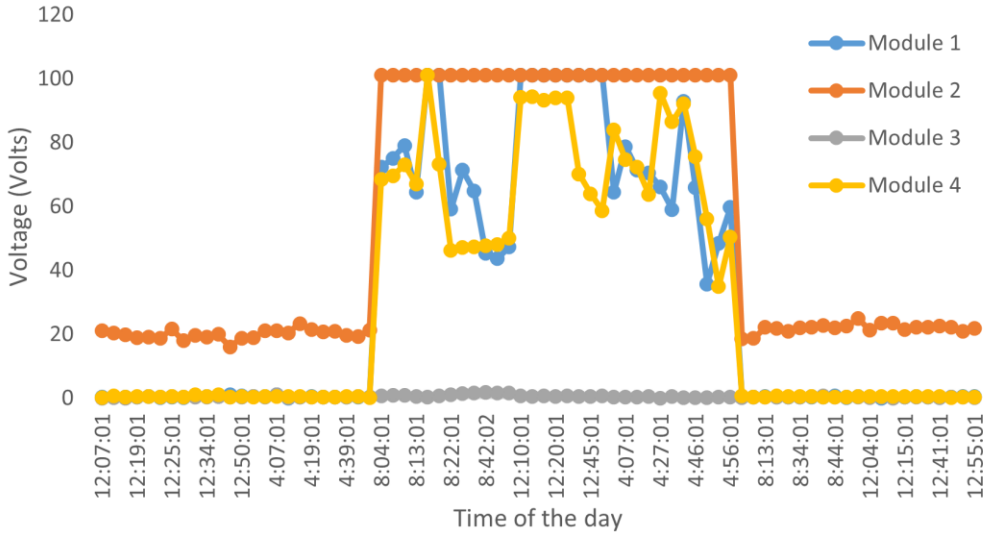

Figure 3.23 Voltage time history from the solar snow fence on Nov 18th, 2023.

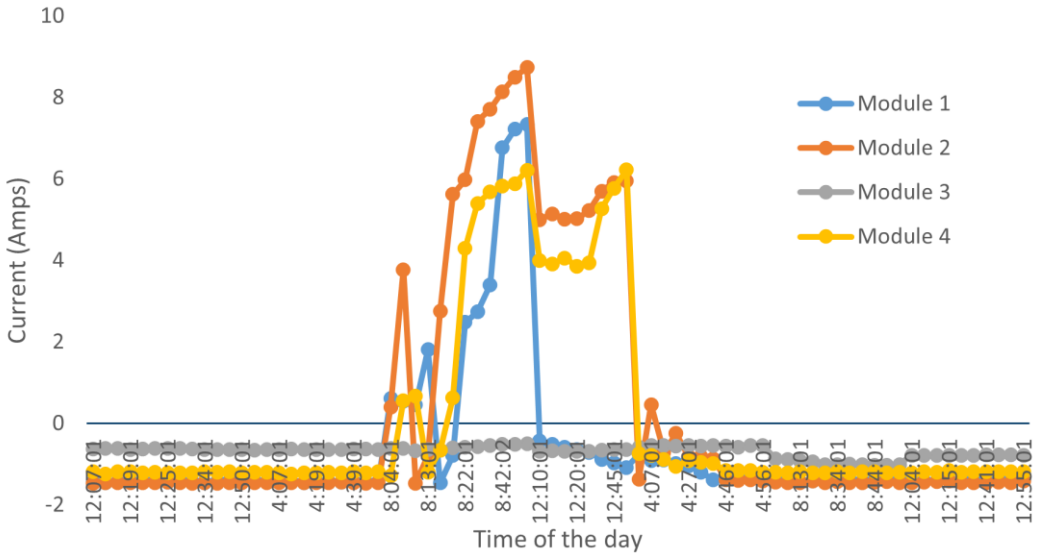

Figure 3.24 Current time history from the solar snow fence on Nov 18th, 2023.

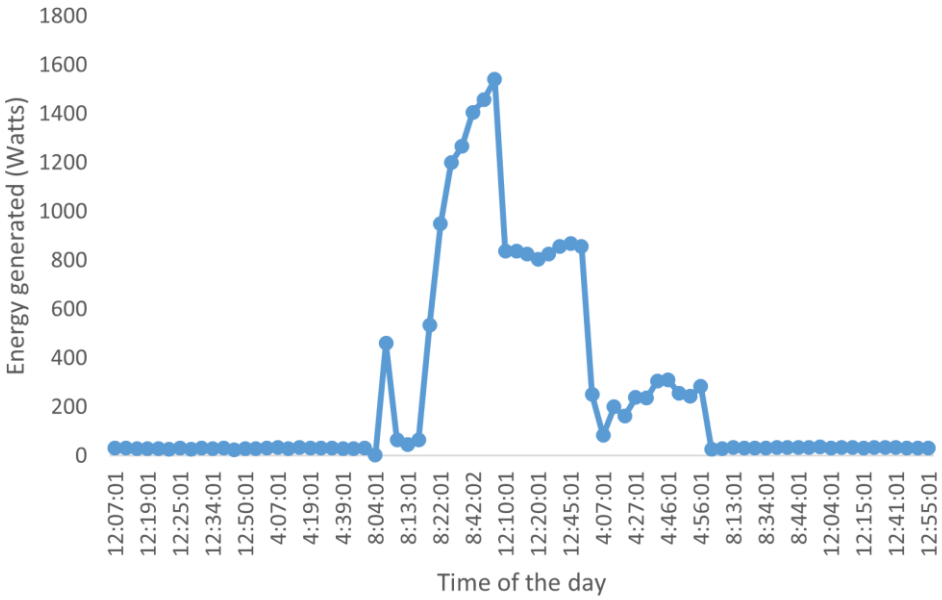

Figure 3.25 Power time history from the solar snow fence on Nov 18th, 2023.

Chapter 4: Field monitoring and cradle to grave life cycle analysis of the solar snow fence implementation

4.1 The field data collected and energy production in the past 5 months

The whole solar snow fence system works with a camera monitoring system, a smart home usage system, a full battery energy storage system, and a data collection system for wind speed, temperature, solar intensity, voltage, and current.

Over the past 6 months, a comprehensive dataset has been gathered for the solar snow fence system including a range of environmental factors. External conditions such as humidity, temperature, solar intensity, and wind speed, provide a holistic perspective on the surrounding environment. Concurrently, the voltage and current data from the solar panels offer insights into the system's performance and energy production. This extensive dataset offers a detailed chronicle of how the solar snow fence interacts with and responds to varying weather conditions throughout the months. It provides valuable information for assessing the system's efficiency, understanding the impact of environmental variables on energy production, and optimizing the overall performance of the solar snow fence in different climatic scenarios.

The raw data obtained from the Pi module produces six files daily, reported at four-hour intervals. These files encapsulate information about external conditions, voltage, and current data. The frequency of readings occurs as often as one minute per data point. Figure 4.1 shows an example of the readings from the Pi module.

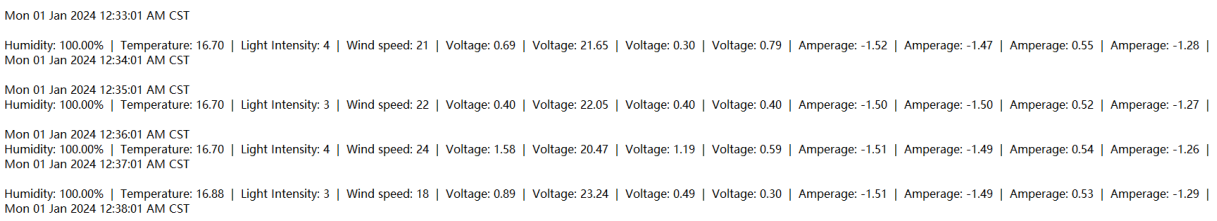

Figure 4.1 Sample Raw data from the Pi module.

In mid-October, 2023, an intermittent system error was identified, occurring during adverse weather conditions that hindered the proper functioning of the system. During such instances, the monitoring module would cease operation, leading to gaps in records and significant time intervals between readings. To address this issue, a solution was implemented by alternating the working schedule of the snow melting pads. This strategy resulted in a notable increase in the frequency of successful readings, mitigating weather-related disruptions and enhancing the system's overall reliability.

From the past 6 months of service, the solar snow fence has worked well without any apparent damage due to wind and snowstorms. The installed snow fence also did not disturb the ongoing traffic from observations. The electricity produced powered the data collection and the monitoring system for the solar snow fence and was used to melt the snow around the control room. The electricity generated during the last 6 months is shown in Figure 4.2. The variation of the energy production is due to the adjustment of the system at the beginning of the project and the variation of the sunlight activities during the past 6 months.

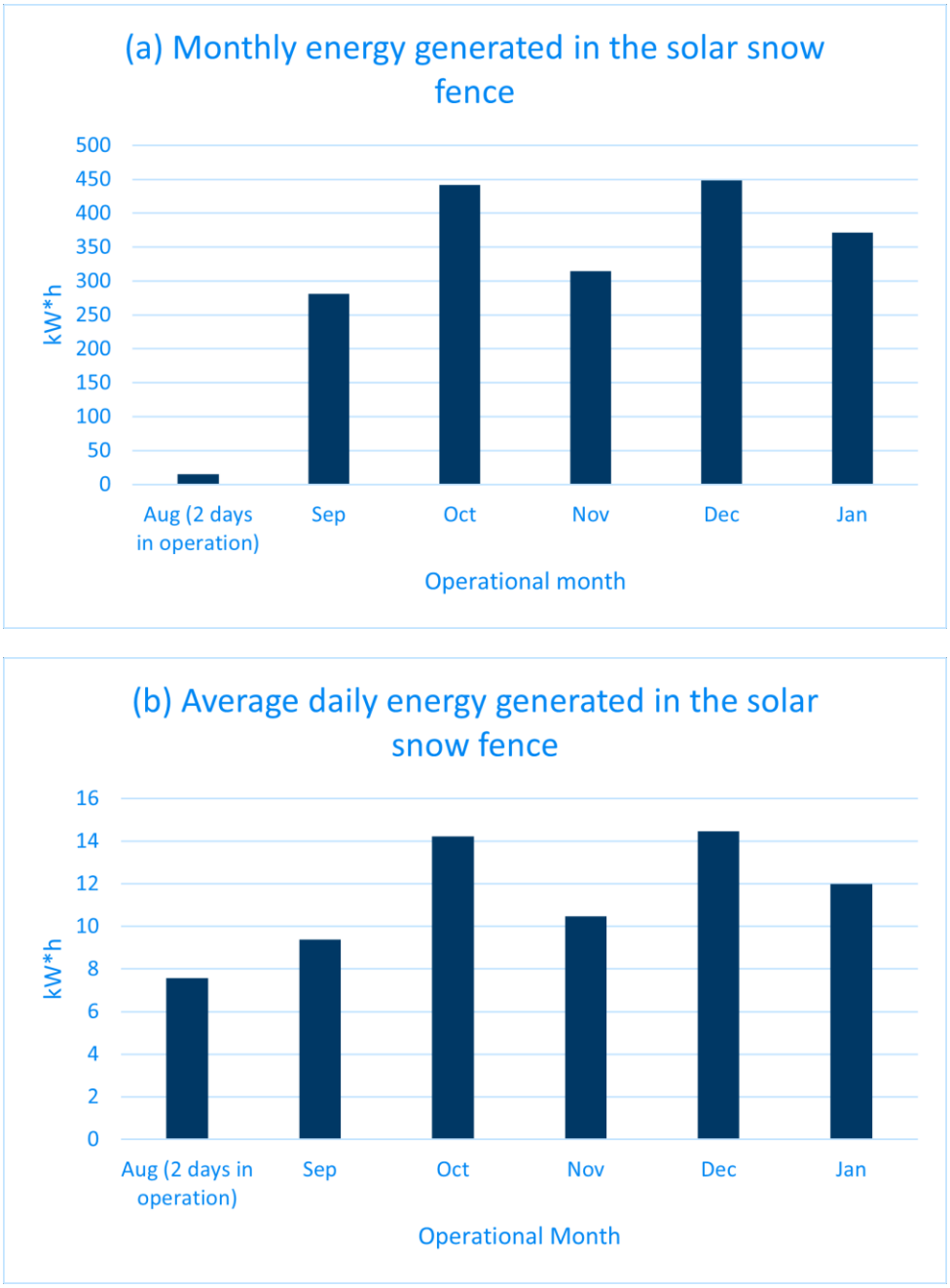

Figure 4.2 The kW*h produced during the past 6 months. (a) Monthly total energy generated, (b) Average daily energy produced.

4.2 Snow depth observations and measurements

Snow depth is also observed for the purpose of comparing the effectiveness of the solar snow fences with the traditional snow fences. A measurement grid is used to map the snow depth around the 220x100-ft area around the snow fence, with 40 ft on the front side of the snow fence (windward side) and 60 ft on the back side of the snow fence (leeward side). Snow depth measurement bar, GPS total station, and GPR are used to measure the snow depth respectively.

4.2.1 Snow depth measured through GPS total stations and snow depth measurement bars

For the GPS total station method, the reference point and the measurement point location will need to be recorded before snow piles up. A site visit was conducted on Oct 15th, 2022 to record these positions (Figure 4.3). A follow-up measurement was conducted on Jan 15th, 2023 and shown in Figure 4.4.

Figure 4.3 Recording of snow depth measurement locations using the GPS total station on Oct 15, 2022.

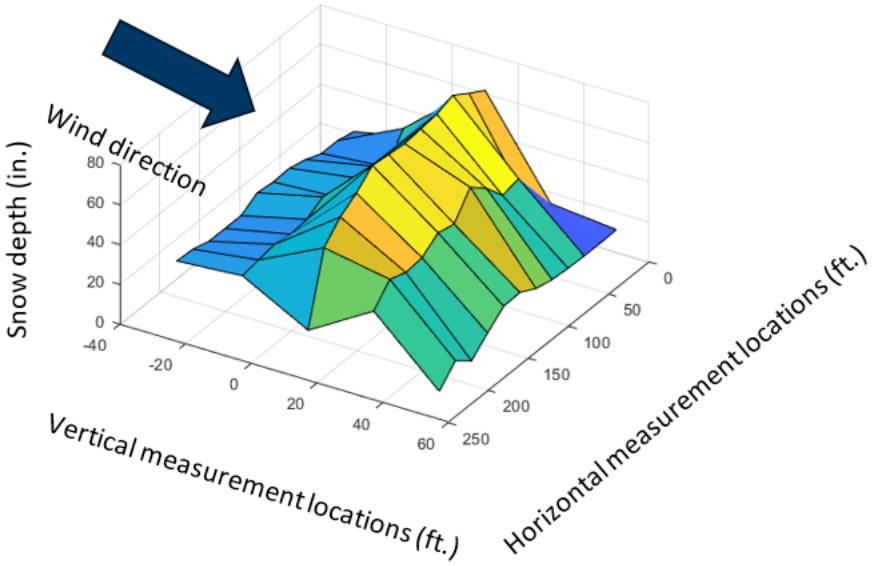

Figure 4.4 Snow depth measurement results on Jan-15-2023 using the GPS total station device and the measurement locations.

The snow depth shows clear separation between the leeward side snow accumulations and the windward side snow accumulation is much less than the leeward side, and the maximum accumulation reaches 82 inches in January of 2023. The end effect is also shown clearly as indicated by the literature. A second visit was conducted on March 5th, 2023 after a large snow event (Figure 4.5). The measurement bar is adopted for this visit and compared with the GPS total station measurements (Figure 4.5). The snow depth measurement result is shown in Figure 4.6. From Figure 4.6, we can see the snow depth has been increased compared to the Jan 15th visit. The maximum snow depth reaches 118 inches. A similar trend is found in the snow depth profile on March 5th, however, a more significant end effect is shown due to the snow removal activities happening at the parking lot nearby.

Figure 4.5 Drift snow profile of the project site on March 5, 2023.

Figure 4.6 Trace the snow depth measurement locations on March 5, 2023.

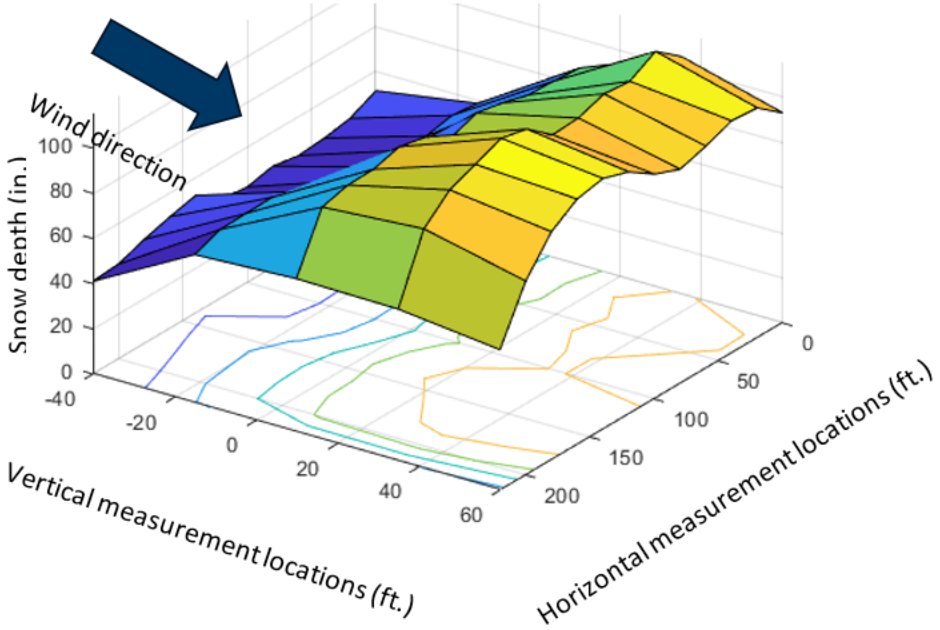

Figure 4.7 Snow depth measurement results on March 5, 2023.

4.2.2 Snow depth measured through Ground Penetrating Radar

Ground-penetrating radar (GPR) is also used to measure snow depth. GPR is a geophysical method that uses electrical magnetic radar pulses to explore the subsurface. It is a non-intrusive method of surveying the sub-surface which is typically used to investigate underground utilities such as concrete, asphalt, metals, pipes, cables or masonry but can be used to measure snow depth as well. The depth that a GPR signal can reach depends on the different types of Antennas used. Some common antenna and the depth they can measure is listed in Table 4.1.

Table 4.1 Common antennas and the depth they can measure

Antenna Type	Depth Range
2600 MHZ High resolution concrete Antenna	0-40 cm (0-12 in)
2300 MHZ Palm XT Antenna	0-60 CM (0-24 in)
2000 MHZ Palm Antenna	0-40 cm (0-12 in)
1600 MHZ General Purpose Concrete Antenna	0-50 cm (0-18 in)
900 MHZ Shielded Antenna	0-1 m (0-3 ft.)
400 MHZ Shielded Antenna	0-4 m (0-12 ft.)
270 MHZ Shielded Antenna	0-6 m (0-18 ft.)

The antenna the research team has is a 1600 MHZ Antenna which can measure snow depth in a range of 0-18 in. A series of testing is conducted to demonstrate its feasibility.

4.2.2.1 Lab detection of bolts under a wood plate

Eight steel bolts were positioned in a series on the ground as shown in Figure 4.8. A ¼ in. thick wooden plate with a length of 5 feet is placed on top of them. The GPR is dragged through the wood plate and the feedback signal is collected and shown in Figure 4.9.

Figure 4.8 Wooden plate and steel bolts.

From Figure 4.9, we can see the reflection due to steel bolts is clearly shown.

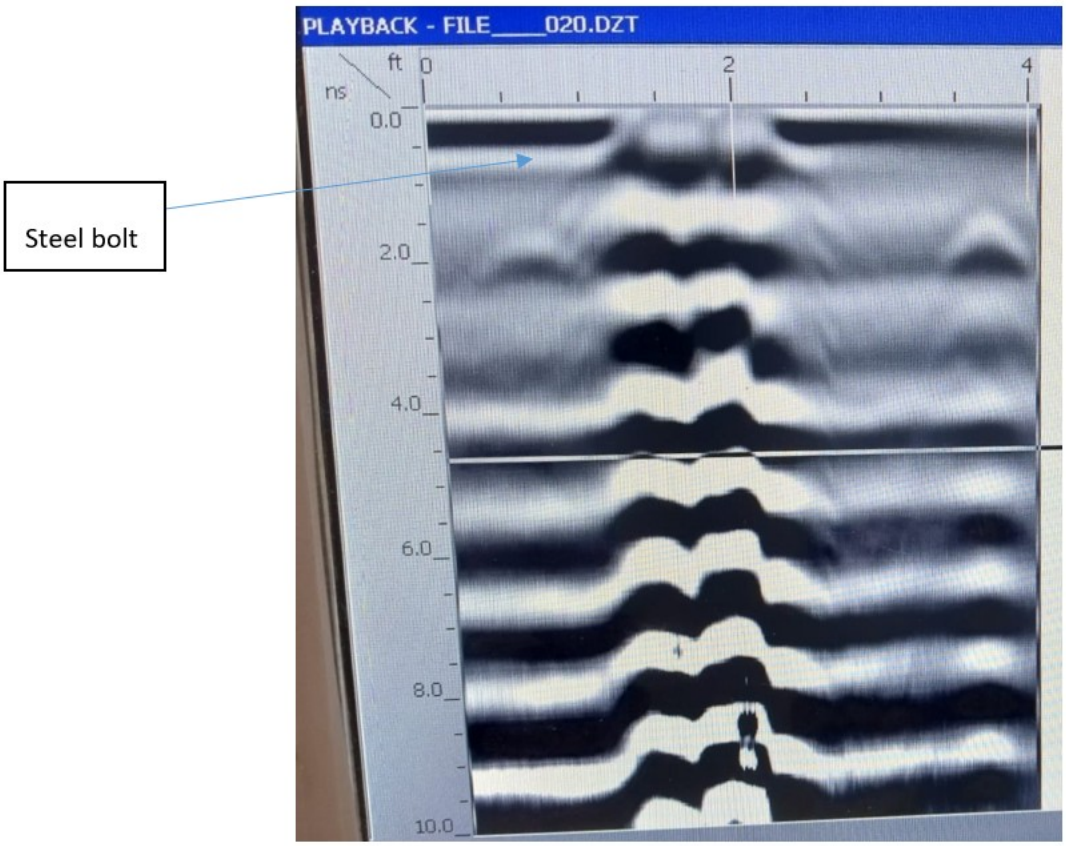

Figure 4.9 The GPR feedback signal obtained for the case that bolts are under a wood plate.

4.2.2.2 Field detection of snow depth

Another test is conducted in a field with snow. The steel bolt was positioned underneath the snow on the surface of a parking lot at NDSU. The reflection depth of the steel bolt will serve as a reference point to check the measured depth. The test setup is shown in Figure 4.10, with the GPR running through the steel bolt perpendicularly. The collected feedback signal is shown in Figure 4.11.

Figure 4.10 6-ft Snow strip used in the snow depth detection test.

From Figure 4.12, a hyperbolic curve is found on the feedback signal which indicates the relative position of the steel bolt with respect to the GPR device. Another layered reflection from the concrete surface is also observed in the photo, which shows a snow depth of around 6 in and a steel bolt buried at a depth of roughly 2.7 inches under the snow.

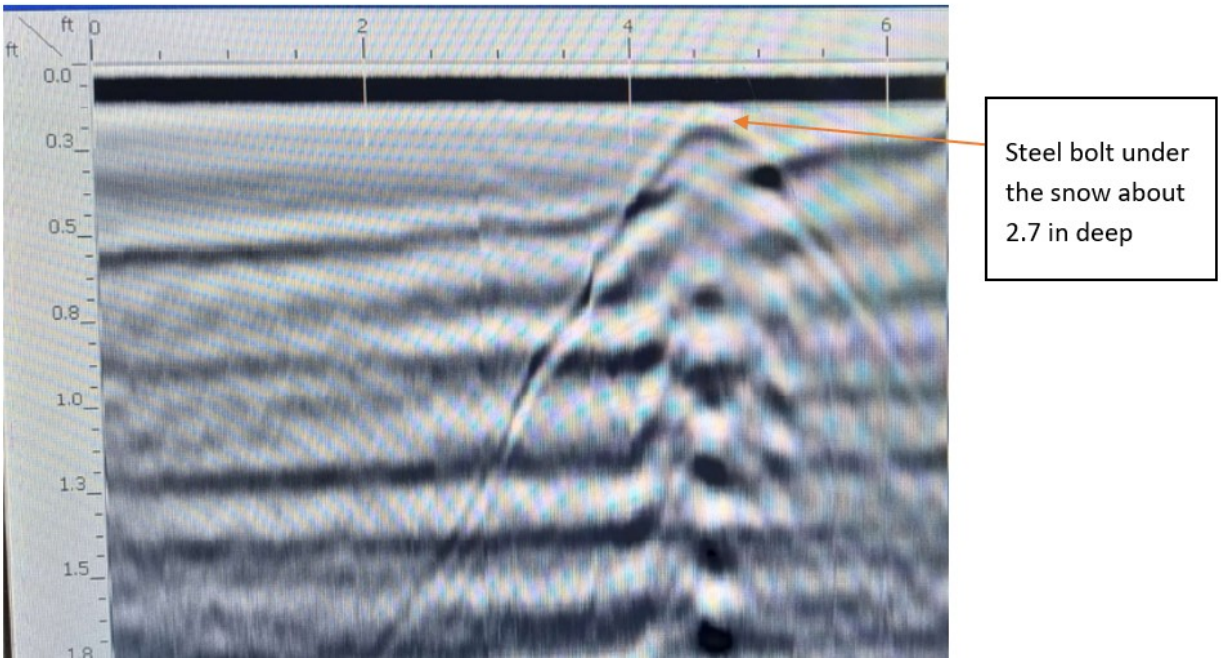

Figure 4.11 GPR feedback signals obtained in this test case.

The tests conducted so far utilized a GPR Antenna operating at 1600 MHz, which allows for a subsurface scan capacity of approximately 18 inches. To measure deep snow depths. it would be necessary to use a 400 MHz Shielded Antenna.

4.2.3 Comparison of snow drifting control efficiency of the solar snow fence vs the traditional snow fence

The snow depths accumulated during the past winter (2023-2024) for both the solar snow fence and the traditional snow fence were monitored and collected (Figures 4.12-4.16). The snow drift formed by the solar snow fence is shown in Figure 4.12, while the leeward drift profile and the windward side drift profiles are shown in Figures 4.13-14. A comparison between the snow drifting control efficiency of the two snow fences is shown in Figures 4.15-16. From Figures 4.15-16, a larger drifted snow was controlled by the solar snow fence compared to the traditional snow fence. This is partially due to the lower porosity of the solar snow fence (42%) compared to the traditional snow fence (50%) and the higher stiffness of the solar snow fence.

Figure 4.12 The drift snow profile formed by the solar snow fence implemented.

Figure 4.13 Comparison of leeward drift snow profiles formed by the solar snow fence and the traditional snow fence.

Figure 4.14 Comparison of windward drift snow profiles formed by the solar snow fence and the traditional snow fence.

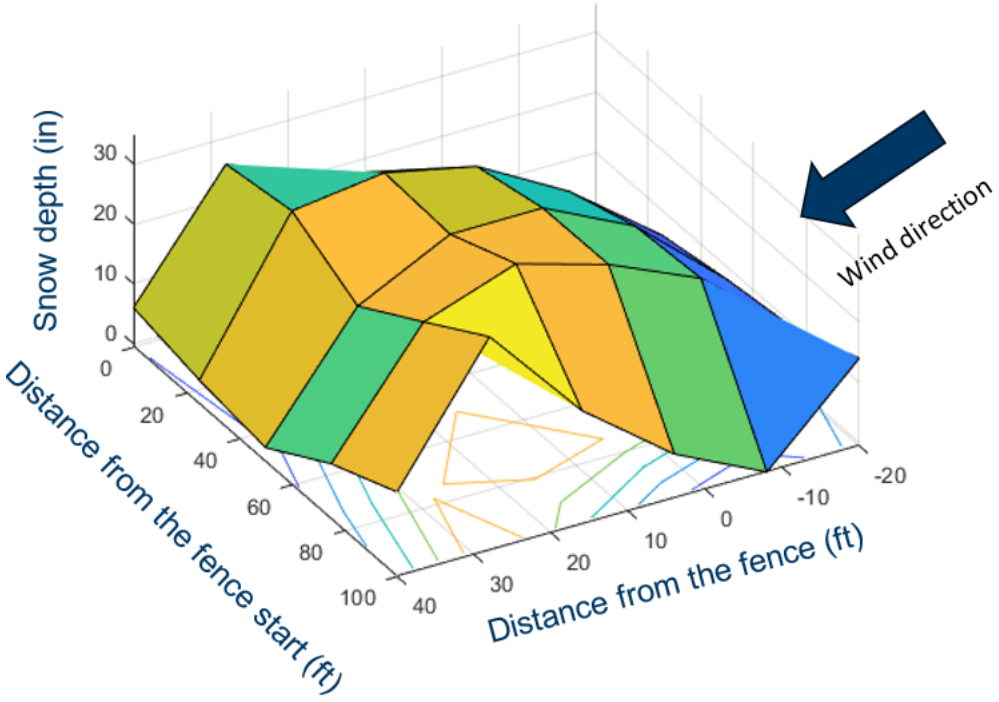

Figure 4.15 Drift snow profile formed by the solar snow fence.

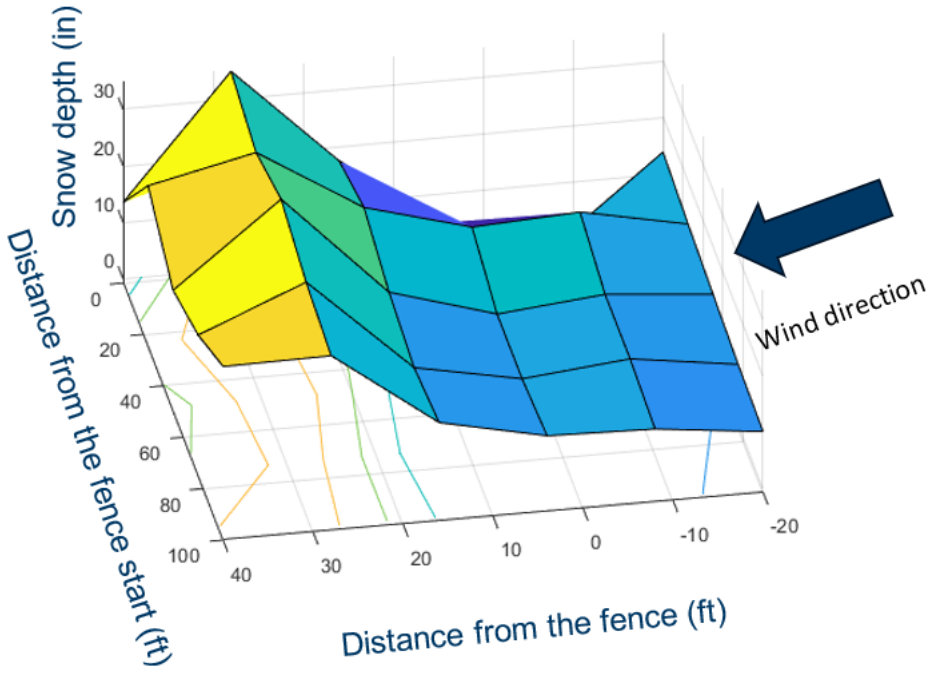

Figure 4.16 Drift snow profile formed by the traditional snow fence.

4.3 The material cost of the solar snow fence system

The material costs associated with the solar snow fence system have been collected. Each component and item within the system has been systematically categorized for further in-depth analysis. This comprehensive approach enables the research team to evaluate and understand the financial implications of the system, facilitating a detailed breakdown of expenses. By categorizing each item, the team can gain insights into the distribution of costs, identify potential areas for optimization, and make informed decisions regarding the economic efficiency of the current solar snow fence system.

Detailed costs of responsive items are stated in Task 4.5 under specific simulations.

4.4 The estimated benefits of the system

The potential benefits of the solar snow fence system are examined from two perspectives:

(a) From the energy produced:

1. The generated photovoltaic (PV) energy is utilized on snow melting pads, ensuring effective and sustainable snow removal (Efficient Snow Melting).
2. The produced energy can be sold to residential areas for household usage, creating a potential revenue stream and contributing to the economic viability of the system (Commercial Viability).
3. Exploring grid connection options enables the system to contribute renewable energy to a larger power grid, supporting broader sustainability goals and potential earning incentives.

(b) From transportation safety/winter road maintenance improved:

The integration of the PV system with a snow fence and the usage of the energy produced on snow-melting pads in Glyndon, MN have positively impacted road conditions in the research area. Snow melting pads, powered by the solar snow fence system, provide an efficient and sustainable solution for snow removal. By utilizing renewable energy for snow melting, drifted snow on roads has been reduced and road conditions have been improved, ensuring safer and more accessible transportation routes during winter weather.

This innovative approach not only addresses snow accumulation but also contributes to the overall maintenance and safety of the road infrastructure. Reduced snow and ice accumulation on the roads can minimize the need for traditional snow removal methods, such as plowing and salting, which have environmental implications. The use of renewable energy for snow melting aligns with sustainable practices and demonstrates a forward-thinking approach to address winter road maintenance challenges.

Table 4.2 lists the benefits identified by MnDOT. Numerical evaluation of these benefits is integrated into the calculator developed by the research team.

Table 4.2 The quantitative benefit generated in this project

Benefit type	Estimated benefit in dollars	Comments/notes
Drifting snow removal savings ($/mile/year)	$34,486.03	Agency cost savings for drifting snow removal
Reduced salt usage (Ice removal) savings ($/mile/year)	$10,207.09	Agency cost savings due to reduced salt usage and sprays.
Reduced crash incident savings ($/mile/year)	$29,638.00	Cost savings from fatal, injury, and property damages due to car crashes
Reduced traffic delay savings ($/mile/year)	$12,826.93	Saving caused by travel time reductions due to improved road conditions
Reduced carbon emission savings ($/mile/year)	$241.40	Cost savings caused by less fuel used in snow removal and salt spray
Salvage values ($/foot)	$0.09	Savings received from steel pole recycling (Scrapmonster)

4.5 The projected cost-benefit analysis of the system for different fence lengths, different years, and different usage approaches

The cost-benefit analysis includes material, labor, and recycling/disposal costs for the installation and maintenance of the PV Snow Fences (PVSF). The benefits include the collected solar energy, i.e., the economic benefit when the generated energy is used by MnDOT facilities with the intention of reducing electricity bills and/or generating revenue for MnDOT by selling the generated power to utility companies. The environmental benefits are also tracked, including the reduced use of fossil fuels to generate the same amount of electrical energy, as well as the associated reduction of greenhouse-gas emissions, the reduction of salt usage for snow and ice control, and the reduction of operations for snow and ice removal. The monetary values of these environmental benefits are reflected in the cost-benefit analysis, and the possible increase for the operation and/or maintenance costs of the snow fences due to the installation and use of solar panels is taken into account. Additionally, the difference between MnDOT's direct ownership and a third-party ownership of the PV system through a Power Purchase Agreement (PPA) is identified and evaluated.

A PPA is a financial mechanism that allows MnDOT to accrue the benefits of solar power without owning the system. In a PPA, a solar project's developer procures, builds, operates, and maintains the solar system while MnDOT buys power from the developer at a negotiated rate (NREL, 2016a). A PPA also allows MnDOT to benefit indirectly from tax incentives through lower electricity prices by using tax equity.

A comprehensive cost-benefit model consists of two sub-models: the models for the snow fences and the PV system. The two models were developed separately, and then, model integrations were conducted. The development of the two models is described in the following sections.

4.5.1 Model for the PV System

In the cost-benefit model for the PV system, the total cost includes the direct capital cost, the indirect capital cost, the operation and maintenance (O&M) cost, and the future cost of the PV system, as shown in Figure 4.17; the total benefits include the solar energy collected, e.g., the economic benefit when the energy is used to power facilities with the intention of reducing electricity bills and/or to generate revenue for MnDOT by selling the generated power to utility companies (Figure 4.18). The environmental benefits' monetary values, e.g., the reduced use of fossil fuels to generate the same amount of electrical energy and/or the associated reduction of greenhouse-gas emissions, were also included. Incentives from federal/state/local governments and/or utility companies, such as the federal solar investment tax credit (ITC; TruNorth Solar), were considered, too. Renewable Energy Certificates (RECs) can also be considered as an additional benefit for the project, if applicable; through the Minnesota Renewable Energy Standard (RES) program, MnDOT can sell the RECs to utility companies (MnDOC, 2019). For example, the RES requires that Xcel Energy obtain 25% of its Minnesota retail sales from renewables, and all other utilities are subject to the RES requirements to obtain 17% of their Minnesota retail sales from renewables. Additionally, in 2013, a Solar Energy Standard (SES) was established, which sets a goal for public utilities, including Minnesota Power, Ottertail Power Company, and Xcel Energy, to obtain at least 1.5% of their total Minnesota retail sales from solar energy by the end of 2020 and 10% by 2030 (MnDOC, 2019).

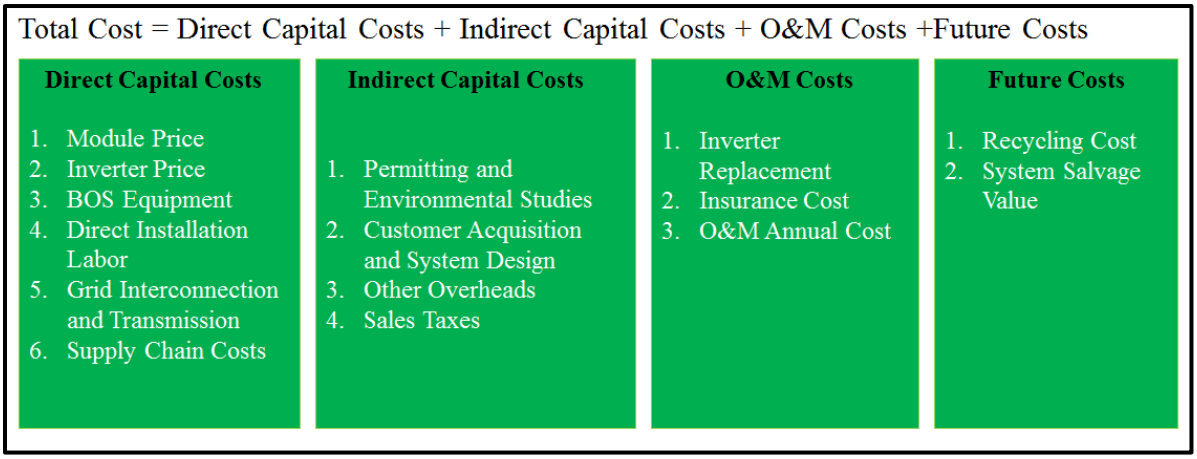

Figure 4.17 Total cost of the PV system (Yang et al., 2021).

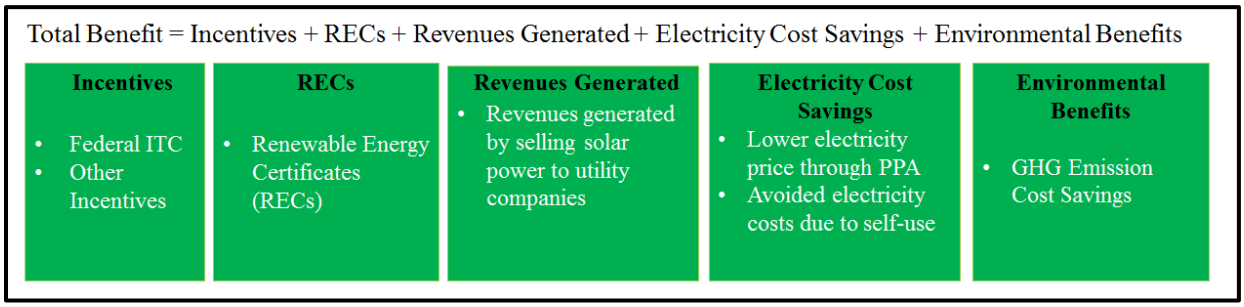

Figure 4.18 Total benefit of the PV system (Yang et al., 2021).

To develop the cost-benefit model of the PV system, several important factors are considered:

- Factor 1: the system's scale/size (i.e., the system's capacity in terms of W or kW), which is determined by the number of PV panels to be installed on the snow fences;
- Factor 2: who has ownership, i.e., direct MnDOT ownership or third-party ownership through a PPA;
- Factor 3: how the generated electrical power is used, i.e., sell it to a utility company or self-use it by MnDOT for existing facilities, such as amenities at highway rest areas or street lights;
- Factor 4: if environmental and/or social benefits are monetarily quantified and included in the analysis? Some of the environmental/social benefits, i.e., the possible reduction of greenhouse-gas emissions, are difficult for MnDOT to monetize and use them directly in order to offset the costs;
- Factor 5: if incentive(s) is(are) included? The current incentive programs may change in the future when/after MnDOT initiates the project.

Given the five critical factors, possible changes for the model are shown in Table 4.3, where 10 different case scenarios are considered. Other conditions and assumptions used to develop the PV cost-benefit model are summarized in Tables 4.4, 4.5, and 4.6.

Table 4.3 Case Scenarios

Factor	Case 1	Case 3	Case 5	Case 7	Case 9
1	100 ft or 1 mile	100 ft or 1 mile	100 ft or 1 mile	100 ft or 1 mile	100 ft or 1 mile
2	Owned by MnDOT	Owned by MnDOT	Owned by MnDOT	Owned by MnDOT	3rd party via PPA
3	Sell to Utility	Sell to Utility	Self-Used	Self-Used	Solar PPA
4	Not Included	Not Included	Not Included	Not Included	Not Included
5	Not Included	Included	Not Included	Included	N/A
Factor	**Case 2**	**Case 4**	**Case 6**	**Case 8**	**Case 10**
1	100 ft or 1 mile	100 ft or 1 mile	100 ft or 1 mile	100 ft or 1 mile	100 ft or 1 mile
2	Owned by MnDOT	Owned by MnDOT	Owned by MnDOT	Owned by MnDOT	3rd party via PPA
3	Sell to Utility	Sell to Utility	Self-Used	Self-Used	Solar PPA
4	Included	Included	Included	Included	Included
5	Not Included	Included	Not Included	Included	N/A

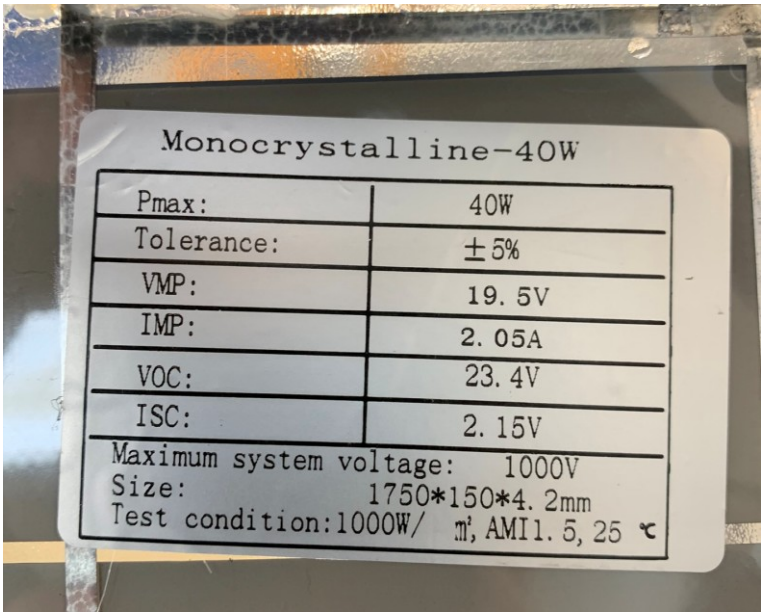

Figure 4.19 Data of the PV panel purchased.

Table 4.4 PV panel information for the 100-ft snow fences

PV Panel Information for Snow Fences		Comments/Notes
Panel Capacity [Watt]	40	Rated power of the PV panel purchased (Figure 4.19)
Panel Length [feet]	6	Actual dimension of the PV panels purchased
Panel Width [feet]	0.5	Actual dimension of the PV panels purchased
Number of Panels per 100 ft	112	Seven customized panels (0.5×6 ft) per section, installed vertically on snow fences (Figure 3.6)
Degradation Rate [%]	0.8	(NREL, 2012)
Array Type	Fixed	Not adjustable to not influence the original function and effectiveness of the snow fences
Tilt [deg]	90	Vertical installation as shown in Figure 3.6
Azimuth [deg]	180	Facing South
Latitude	46.88° N	Actual installation location (Figure 3.1)
Longitude	96.66° W	
Annual AC Energy Output: 100 ft [kWh]	2,869	Calculated based on the actual measurements (for 6 months) and by using the online PV Watts Calculator developed by NREL (Pvwatts) for the other 6 months (as shown in Figure 4.2)
Metric Tons of CO2 Equivalent/year: 100 ft	2	Calculated by using the EPA Greenhouse Gas Equivalencies Calculator (National Average) (U.S. EPA)

Table 4.5 Cost information for the PV system

PV System's Cost Information		Comments/Notes
Direct Capital Costs		
Module Price [$/W]	$1.25	Based on the actual purchasing price
Inverter Price [$/W]	$0.20	(NREL, 2016b)
Balance-of-System (BOS) Equipment [$/W]	$2.09	(NREL, 2016b)
Direct Installation Labor [$/W]	$0.30	(NREL, 2016b)
Grid Interconnection and Transmission [$/W]	$0.07	(NREL, 2016b)
Supply Chain Costs [% of the total material cost]	10%	(NREL, 2018a)
Total Direct Capital Costs [$/W]	$4.26	-
Indirect Capital Costs		
Permitting and Environmental Studies [$/W]	$0.06	(NREL, 2016b)
Customer Acquisition and System Design [$/W]	$0.08	(NREL, 2016b)
Other Overheads [$/W]	$0.30	(NREL, 2016b)
Sales Taxes [%]	6.875%	(Taxmaps)
Total Indirect Capital Costs [$/W]	$0.69	-
O&M Costs		
Inverter Lifetime [Years]	13	(NREL, 2016b)
Inverter Replacement [$/W]	$0.11	(NREL, 2018a)
Insurance Cost by Capacity [$/kW-yr]	$6.70	(Enbar et al., 2016)
O&M Annual Cost by Capacity [$/kW-yr]	$12.27	(NREL, 2016b)
Total O&M Costs [$/W]	$0.47	-
Future Costs		
Recycling Cost [$/W]	$0.17	(Fthenakis , 2000)
System Salvage Value [% of Capital Cost]	15%	(Guney & Onat, 2010)
Financial Parameters		
PV System's Lifetime [Year]	25	-
Real Discount Rate [%/yr]	5.5%	(Federal Reserve, 2024)
Federal Income Tax Rate [%]	0.00%	Confirmed by MnDOT
State Income Tax Rate [%]	0.00%	Confirmed by MnDOT
Electricity Utility Price Paid by MnDOT* [$/kWh]	$0.12	According to the utility costs provided by MnDOT
Li-ion Standalone Storage System Cost (For Self-Use)		
Duration [hr]	2	-
Li-ion Battery Cost [$/kWh]	$209.00	(NREL, 2018b)

PV System's Cost Information		Comments/Notes
Battery's Central Inverter [$/W]	$0.07	(NREL, 2018b)
Structural BOS [$/W]	$0.03	(NREL, 2018b)
Electrical BOS [$/W]	$0.10	(NREL, 2018b)
Installation Labor & Equipment [$/W]	$0.07	(NREL, 2018b)
EPC Overhead [$/W]	$0.03	(NREL, 2018b)
Land Acquisition [$/W]	$0.01	(NREL, 2018b)
Permitting Fee [$/W]	$0.01	(NREL, 2018b)
Interconnection Fee [$/W]	$0.03	(NREL, 2018b)
Contingency [$/W]	$0.02	(NREL, 2018b)
Developer Overhead [$/W]	$0.02	(NREL, 2018b)
EPC/Developer Net Profit [$/W]	$0.04	(NREL, 2018b)
PV Cost Summary		
PV for 100-ft Snow Fences [$/W]	$4.95/$5.85	System Size: 4,480 W $4.95/W for selling power to a utility company $5.85/W for self-use (including battery costs)

Table 4.6 Benefit information for the PV system

PV System's Benefit Information		Comments/Notes
Federal ITC or other incentives	10.00%	(U.S. DOE, 2021)
RECs* [$/REC or $/MWh]	$0.65	(MnDOC, 2019)
Price to sell back to a utility company [$/kWh]	$0.11	(Yang et al., 2021)
PPA for 3rd-party ownership [$/kWh]	$0.10	(NREL, 2016a)
Bituminous Coal [Per Short Ton]		
Heating Value [MMBtu]	24.93	(U.S. EPA, 2014)
1 kWh to Btu	3,412	(U.S. EIA)
Electricity Output [kWh]	7306.57	(U.S. EPA, 2014)
kg CO_2	2,325	(U.S. EPA, 2014)
g CH4	274	(U.S. EPA, 2014)
g N2O	40	(U.S. EPA, 2014)
Greenhouse gas (GHG) Emission Cost Savings		
Per metric ton CO_2	$42.00	(U.S. EPA, 2017)
Per metric ton CH4	$1,200.00	(U.S. EPA, 2017)
Per metric ton N2O	$15,000.00	(U.S. EPA, 2017)
GHG Emission Ratio (Coal/Solar)	8.37	(Fan, 2014)

4.5.2 Model for Snow Fences

Table 4.7 shows the cost information for the snow fences used in the analysis, and the benefit information is shown in Table 4.2.

Table 4.7 Cost information for the structural snow fences

Structural Snow-Fence Cost Information		Comments/Notes
Unit Hight [feet]	8	Based on actual installation (Figure 3.6)
Unit Length [feet]	100	-
Install & Material Costs [$/foot]	$153.20	Based on actual installation of the steel posts (about 6 feet apart)
Land Cost [$/linear foot/year]*	$1.00	Rental cost (Provided by MnDOT)
O&M Cost [$/Year]	$3,000.00	Including the cost of lawn mowing for safety purposes around the PVSF
Property Tax	$0	Lease: Paid by landowners
Recycling Cost [$/foot]	$0.50	(Ernie's Wagon)
Real Discount Rate* [%]	5.5%	(Federal Reserve, 2024)

4.5.3 Model Integration Between PV Panels and Structural Snow Fences

Integrating the developed models for PV panels and snow fences was done, where the cash flows for the PV panels and the structural snow fences are integrated mathematically by adding the corresponding costs and benefits which are incurred in the same year together, but with the exception that the snow-fence rails are replaced with the customized PV panels as shown in Figure 3.6.

In this analysis, four different studies are included, as listed below, and the differences between these four studies are detailed in Table 4.8.

- Study 1 – The results from the 1-Mile PVSF model in the Phase I project (Yang et al., 2021)
- Study 2 – The results from the 1-Mile PVSF model in the Phase I project (Yang et al., 2021) but with the interest rate changed from 0.35% to 5.5%
- Study 3 – The results from the 100-ft PVSF model established in this Phase II project using the real installation and operation data, as described from Tables 4.2 and 4.4 to 4.7.
- Study 4 – The results from a model similar to the one used in Study 3 but for an ideal case where the length of the PVSF project is changed to 1 mile, the size of the PV panel becomes 12'× 0.5', and eight PV panels are installed between two steel posts.

Table 4.8 Parameter comparison among the four analysis studies

	Study No.			
	1	2	3	4
Interest Rate (%)	0.35%	5.5%	5.5%	5.5%
Project Length	1 Mile	1 Mile	100 ft	1 Mile
Panel Capacity [Watt]	100	100	40	80
Panel Length × Width [feet]	12×0.5	12×0.5	6×0.5	12×0.5
Number of Panels	3,520	3,520	112	3,520
Module Cost ($/Watt)	0.85	0.85	1.25	1.02
Inverter Cost ($/Watt)	0.15	0.15	0.20	0.20
BOS Equipment Cost ($/Watt)	0.35	0.35	2.09	1.71
Direct Installation Labor ($/Watt)	0.20	0.20	0.30	0.20
Grid Interconnection and Transmission ($/Watt)	0.05	0.05	0.07	0.05
Permitting and Environmental Studies ($/Watt)	0.05	0.05	0.06	0.05
Customer Acquisition and System Design ($/Watt)	0.05	0.05	0.08	0.05
Other Overheads ($/Watt)	0.20	0.20	0.30	0.20
Inverter Replacement ($/Watt)	0.09	0.09	0.11	0.09
Insurance Cost by Capacity ($/kW-yr)	5.00	5.00	6.70	5.00
O&M Annual Cost by Capacity ($/kW-yr)	10.00	10.00	12.27	10.00
DC System Size (kW)	352	352	4.48	281.6
Annual AC Energy Output (kWh)	352,348*	352,348*	2,869**	281,894*
Snow Fence Installation Cost ($/ft)***	72.10	72.10	153.20	72.10
Snow Fence Recycling Cost ($/ft)	0.25	0.25	0.50	0.25

*Estimated using (Pvwatts); **Calculated based on the actual measurements (for 6 months) and by using (Pvwatts) for the other 6 months; ***Material and installation costs for steel posts (the number of the posts depends on the size of the PV panel, i.e., the number of posts in Study 3 is nearly doubled compared to that in Study 1, 2, and 4.

4.5.4 Results and Discussions

Tables 4.9 and 4.10 summarize the cost-benefit analysis results between Study 1 and 2 and Study 3 and Study 4, respectively. Three different methods were used to compare these results**: *Payback Period (PP)*, *Net Present Value (NPV)*,** and ***Internal Rate of Return (IRR)***.

Table 4.9 Results between Study 1 and 2

Study 1 (1 Mile – 0.35%)					Study 2 (1 Mile – 5.5%)				
Case Scenario	NPV	PP (Yr)	IRR	Rank*	Case Scenario	NPV	PP (Yr)	IRR	Rank*
Case 10	$1,823,048.67	4	28.79%	1	Case 10	$889,195.29	4	28.80%	1
Case 9	$1,731,952.54	4	27.48%	2	Case 9	$837,003.91	5	27.48%	2
Case 4	$1,674,543.71	9	10.58%	3	Case 4	$523,443.51	12	10.58%	3
Case 2	$1,599,715.11	10	9.61%	4	Case 3	$468,396.52	13	10.08%	4
Case 3	$1,578,463.31	10	10.08%	5	Case 2	$448,614.91	14	9.61%	5
Case 1	$1,503,634.71	10	9.13%	6	Case 1	$393,567.92	15	9.13%	6
Case 8	$1,466,940.25	11	7.73%	7	Case 8	$283,091.62	18	7.73%	7
Case 7	$1,370,859.85	12	7.31%	8	Case 7	$228,044.63	19	7.31%	8
Case 6	$1,360,524.49	12	6.81%	9	Case 6	$176,675.86	20	6.81%	9
Case 5	$1,264,444.09	13	6.41%	10	Case 5	$121,628.87	21	6.41%	10

*Rank is based on the NPV.

Table 4.10 Results between Study 3 and 4

Study 3 (100 ft – Real Power Generation)					Study 4 (1 Mile – Ideal Case Based on Actual Data)				
Case Scenario	NPV	PP (Yr)	IRR	Rank*	Case Scenario	NPV	PP (Yr)	IRR	Rank*
Case 10	$8,678.39	11	11.85%	1	Case 10	$861,183.99	5	28.09%	1
Case 9	$8,253.44	11	11.56%	2	Case 9	$819,430.89	5	27.03%	2
Case 4	-$9,401.21	>25	2.27%	3	Case 4	$102,456.98	22	6.29%	3
Case 3	-$9,849.41	>25	2.10%	4	Case 3	$58,419.38	23	5.96%	4
Case 2	-$11,617.72	>25	1.71%	5	Case 2	-$9,406.86	>25	5.43%	5
Case 1	-$12,065.92	>25	1.54%	6	Case 1	-$53,444.46	>25	5.11%	6
Case 8	-$12,661.68	>25	1.50%	7	Case 8	-$89,824.53	>25	4.89%	7
Case 7	-$13,109.87	>25	1.34%	8	Case 7	-$133,862.13	>25	4.58%	8
Case 6	-$15,280.21	>25	0.93%	9	Case 6	-$226,958.10	>25	4.05%	9
Case 5	-$15,728.40	>25	0.77%	10	Case 5	-$270,995.69	>25	3.76%	10

*Rank is based on the NPV.

Study 1 serves as a benchmark for understanding the potential outcomes under standard conditions, which offers a theoretical perspective on the cost-benefit dynamics. For example, as shown in Table 4.9 by comparing the results between Study 1 and 2, a decrease in the NPV and an increase of the Payback Period are observed, due to the rise of the interest rate from 0.35% to 5.5%, in accordance with the Federal Reserve guidance (Federal Reserve, 2024). These adjustments aim to provide a more realistic and contextually relevant representation of the solar snow fence system's cost-benefit analysis, accounting for the prevailing economic conditions. A higher discount rate reflects a greater opportunity cost of capital and places more weight on the time value of money. In other words, future cash flows are

worth less in today's terms when discounted at a higher rate. Consequently, the NPV, which represents the net difference between the present value of benefits and costs, decreases.

Table 4.10 shows the analysis results of Study 3 and 4, where Study 3 demonstrates the results of the 100-feet PVSF based on the real installation and operation data. In comparison between Study 2 and 3, a decline is noted in the NPV, IRR, and an increase in Payback Period numbers. Upon careful examination of the patterns, we can derive conclusions regarding the factors that likely contribute to this observed change.

- Increased capital costs, including module, BOS costs, etc. as shown in Table 4.8
- Increased number of steel posts (doubled)
- Increased interest rate from 0.35% to 5.5%
- Designed PV System capacity decreased from 352 kW/mile to 246.4 kW/mile, a 30% decrease.

Study 4 extrapolates from the actual data of a 100-foot PVSF to model a one-mile scenario, showing enhanced financial outcomes in terms of NPV, PP, and IRR. This scale-up demonstrates the economic advantage of larger projects, attributed to economies of scale, as highlighted in the analysis. Specifically, within the context of Solar PPAs for Cases 9 and 10, despite higher interest rates, the project maintains a robust positive NPV and elevated IRRs. This resilience suggests that, even with an increased discount rate, the solar snow fence system's financial assessment remains positive. This positive NPV signifies that the benefits derived from the project (discounted back to their present value) outweigh the associated costs, even in the face of a higher opportunity cost of capital.

4.5.5 Summaries

Profitability: The economic viability of the solar snow fence system varies across different scenarios. Cases 9 and 10, involving both photovoltaic and snow fence components with PPA contracts, show promising financial returns with positive Net Present Values (NPVs) and high Internal Rates of Return (IRRs), indicating potential profitability.

Economies of Scale: The scalability of the project is a critical factor. Larger projects, such as those covering 1 mile, may benefit from economies of scale, potentially reducing costs and enhancing their overall economic performance.

Cost Optimization: Improvement of the system connection between the PV panel and the steel post design will be recommended for cost-effective purposes. Currently, due to the high level of customization of the system, the cost of Module and BOS equipment remains higher than those of the cases using the NREL-referenced estimations. The construction and installation of the solar snow fence system involve helical pier drilling and metal posts, showcasing a comprehensive approach to ensure stability and durability. Efficient logistics management is highlighted as a potential factor for cost reduction.

Chapter 5: Survivability of the solar snow fence year around and integration of snow drift control and melting

5.1 Wind speed and solar intensity in the past year and its impact on the safety of the solar snow fence

In the past year, the wind speed and solar intensity data have been collected in the project site and are compared with the North Dakota Agircultural Weather Network (NDAWN) data. By comparing the wind speed at the project site (Figure 5.1) and the open air wind speed (Figure 5.2), we can see the wind speed at the project site is higher than the open air wind speed recorded by NDAWN (https://ndawn.ndsu.nodak.edu/weather-data-yearly.html), however the overall trend is similar. Local disturbance due to the surrounding buildings may cause this difference. The solar snow fence is designed with a wind speed of 105 mph, which is much higher than the actual measured maximum speed (30 mph) and the monthly average wind speeds. There are no issues of structural failure in theory, and the research team did not observe any structure failure in the past 18 months either.

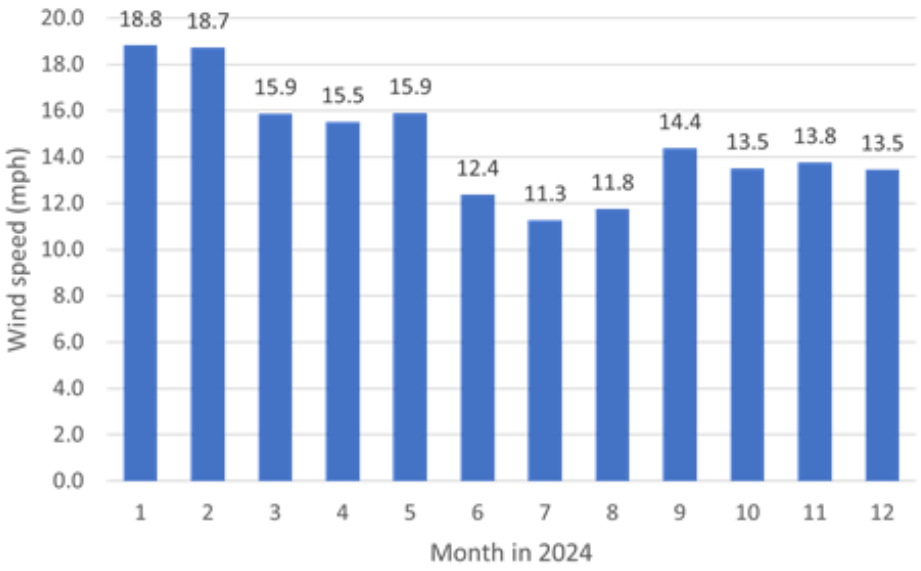

Figure 5.1 Wind speed at the project site, Glyndon, MN.

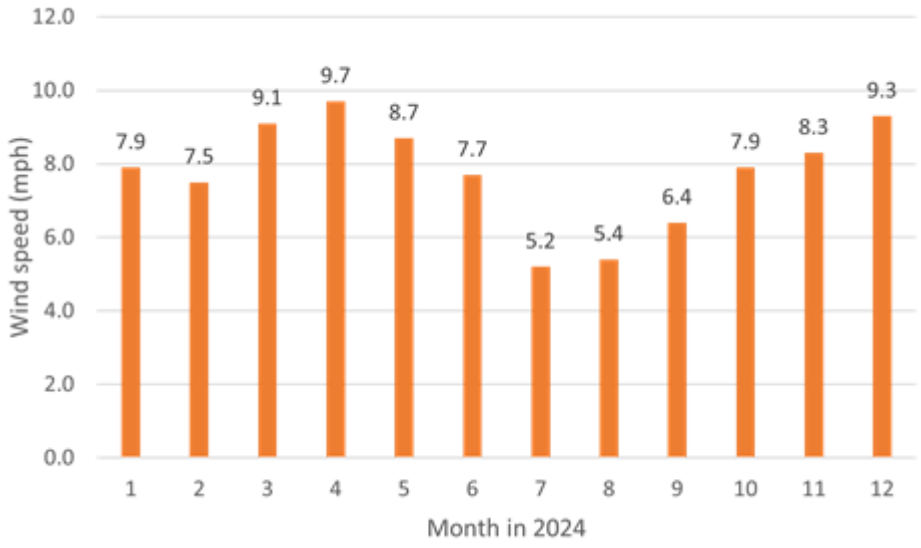

Figure 5.2 Open air wind speed collected for Glyndon, MN through NDAWN.

Solar activity affects energy production of the solar snow fence, which has been monitored and correlated to the energy product on the site. A comparison of the solar intensity on site (Figure 5.3) with the solar intensity provided by NDAWN (https://ndawn.ndsu.nodak.edu/weather-data-yearly.html) (Figure 5.4) shows similar trend, but a large discrepancy is found in December and January of 2024. The overall values measured on site is larger than the data collected by NDAWN most of the months. The main reason may be the incident solar radiation flux density from NDAWN is measured at approximately 7 ft (2 m) above the soil surface with a pyranometer, while the light intensity sensor used in the project uses a reference peak solar irrandiance of 31.2 MJ/m^2 as stated in NDAWN.

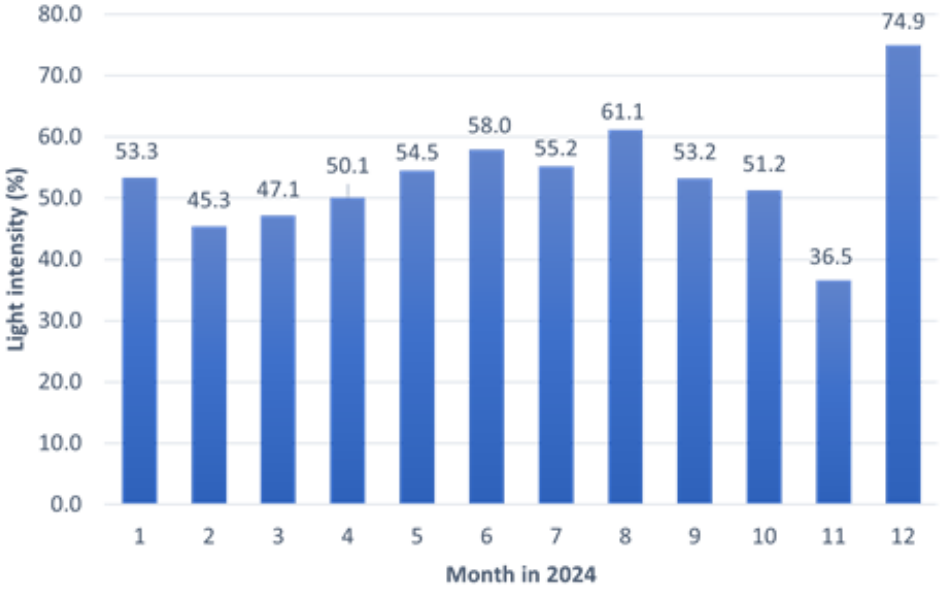

Figure 5.3 Light intensity at the project site, Glyndon, MN.

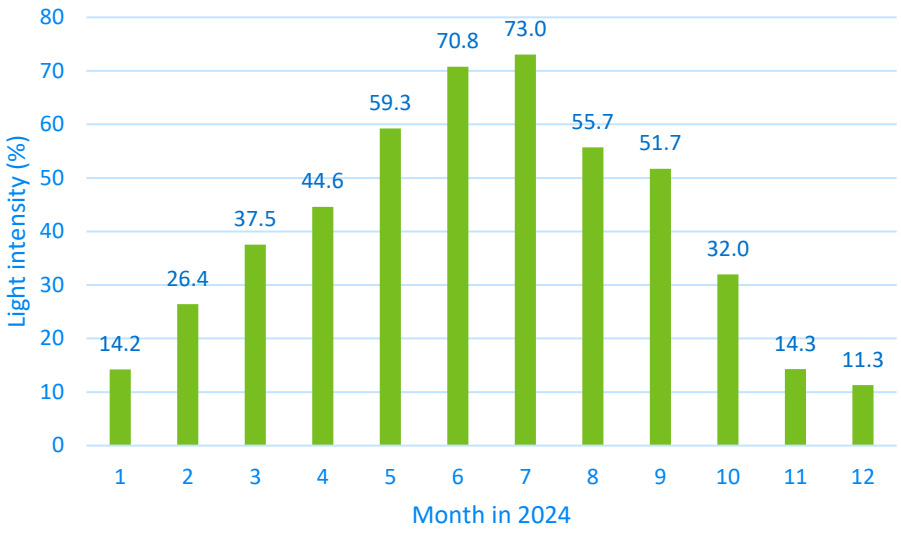

Figure 5.4 Light intensity at Glyndon, MN using the NDAWN data.

5.2 Integration of snow drift control and melting

The solar snow fence has a triple function that includes snow drift control, energy production, and snow melting.

5.2.1 Snow drift control

In snow drift control, a comparison between the drifted snow profile in the 2023-2024 winter season and the 2024-2025 winter season is shown in Figures 4.15-16 and Figures 5.5-10, in which a clear gap is observed in the drifted snow profile of the 2024-2025 winter season. An approximate 5 ft gap is created due to the snow melting pad used in the project. If we compare the drifted snow profile in the 2023-2024 winter season for the solar snow fence and the traditional snow fence (Figure 4.15 and Figure 4.16) , we can see the solar snow fence contains more drifted snow when the snow melting pads are not used. The reason for this result is due to the projected surface of solar panel frame, which further reduces the wind speed behind the fence compared to the traditional structural snow fence. If we compare the drifted snow profile in the 2024-2025 winter season for the solar snow fence and the traditional snow fence (Figure 5.8 and Figure 5.10) when the snow melting pads are used. Similar conclusion as the 2023-2024 season can be drawn. A maximum snow drift height of 30” is reached on the solar snow fence with the snow melting pad compared to the maximum drift height of 26’’ for the traditional structural snow fence on January 22, 2025. moreover, the snow melting pad created a clear 5 ft gap, which further reduces the wind speed behind the fence and facilitate the snow deposition on the drifted profile, as shown in Figure 5. 7, 5.8, 5.9, and 5.10.

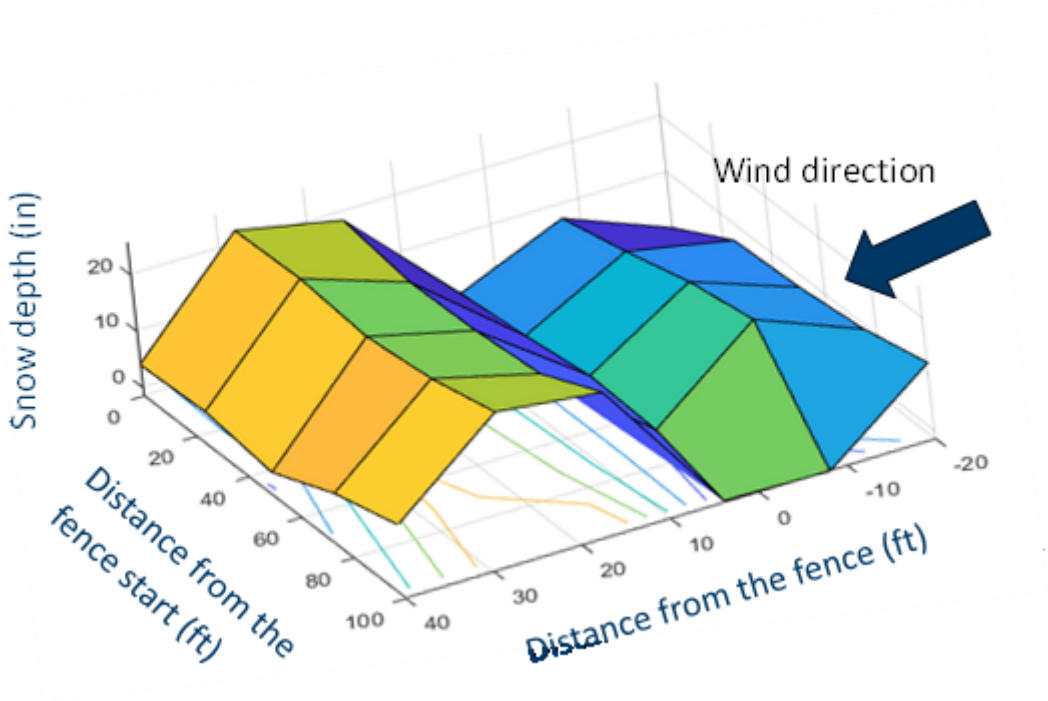

Figure 5.5 Drift snow profile formed by the solar snow fence with snow melting pads on January 22, 2025.

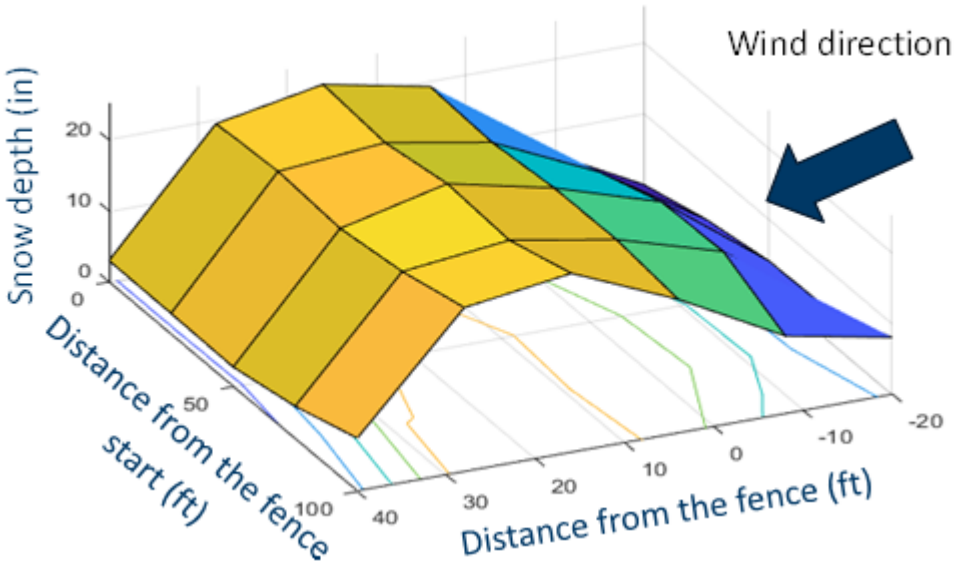

Figure 5.6 Drift snow profile formed by the traditional snow fence on January 22, 2025.

Figure 5.7 Drift snow profile formed by the solar snow fence with the snow melting pads.

Figure 5.8 The melted gap formed by the solar snow fence.

Figure 5.9 Comparison of the drifted snow between the solar snow fence and the traditional snow fence.

Figure 5.10 The drifted snow behind the traditional snow fence.

5.2.2 Energy production and consumption

Energy production has been recorded for 18 months, starting August 2023, which is shown in Figure 5.11 and Figure 5.12. Figure 5.11 shows the monthly energy produced through the 96 ft solar snow fence. We can see an average of more than 319.4 kW*h is produced per month, except August 2024, and January and February of 2025 due to system maintenance.

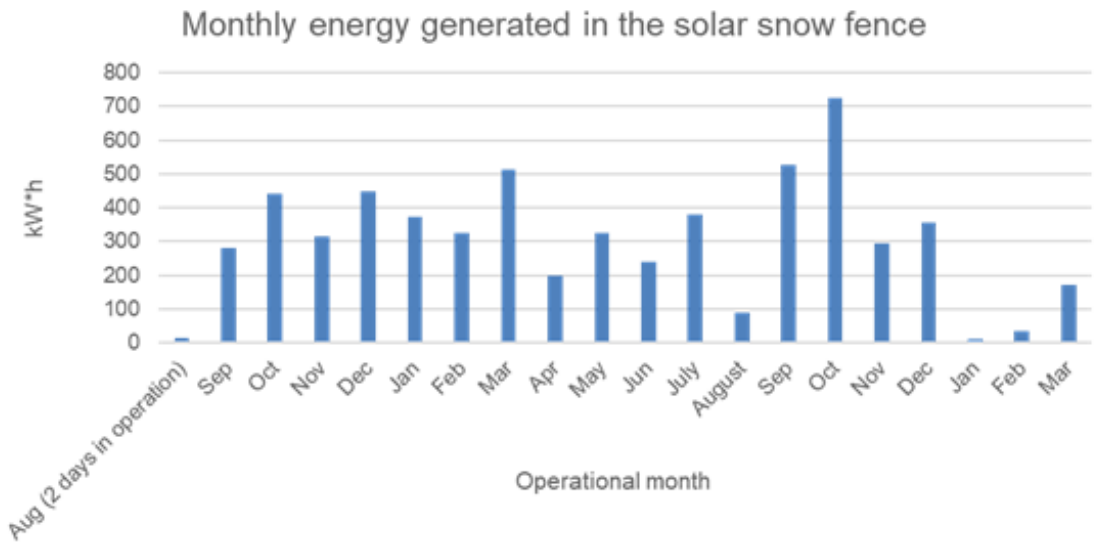

Figure 5.11 Monthly energy produced through the 96' solar snow fence.

Average daily energy produced is also plotted and shown in Figure 5.12. An average daily production of 11.7 kW*h is generated.

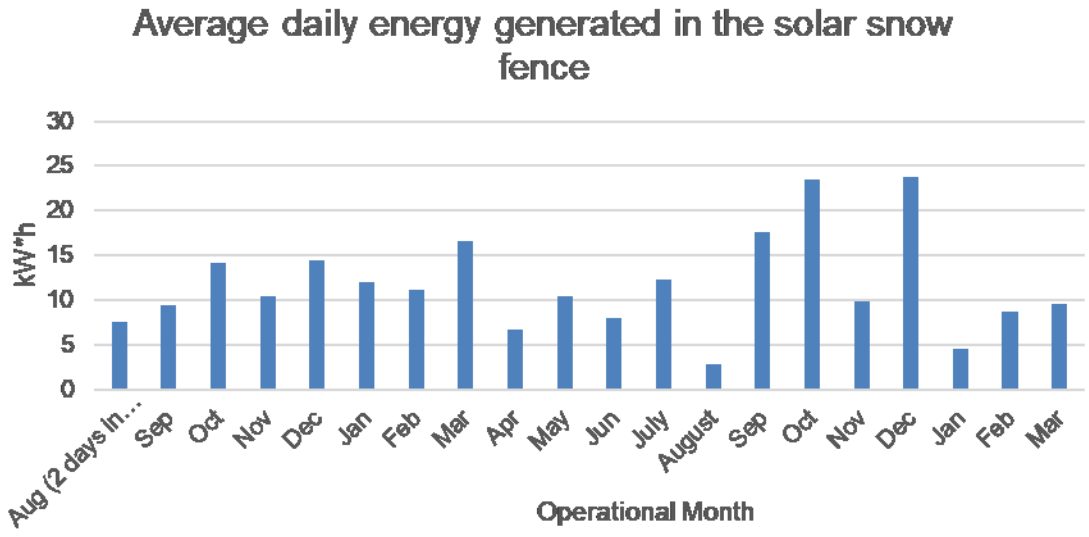

Figure 5.12 Daily avaerge power generated through the 96' solar snow fence.

The energy generated has been used to power the camera to monitor the solar snow fence, the data acqusistion system to collect the temperature, moisture, wind speed, and solar intensity data, and to melt the deposited snow. Sixteen snow melting pads have been purchased and used to melt the snow along the solar fence. Each of the pads is 3x6'. These sixteen melting pads cover the entire 96' long snow fence and is turned on one hour per day to melt the daily average snow precipitation of 2 inch in the Glyndon area. The snow melting activity can be remotely controlled as well.

Snow melting through the snow melting pads consumes 80-90% of the energy produced. Their daily average consumption of the energy is shown in Figure 5.13. Due to less snow precipitation of the 2024-2025 winter season, the snow melting pads were arranged to melt the snow more around the control shed room every day and the remaining pads take turns to be turned on for one hour every 2 days. Their monthly energy consumption in February 2025 is shown in Figure 5.14.

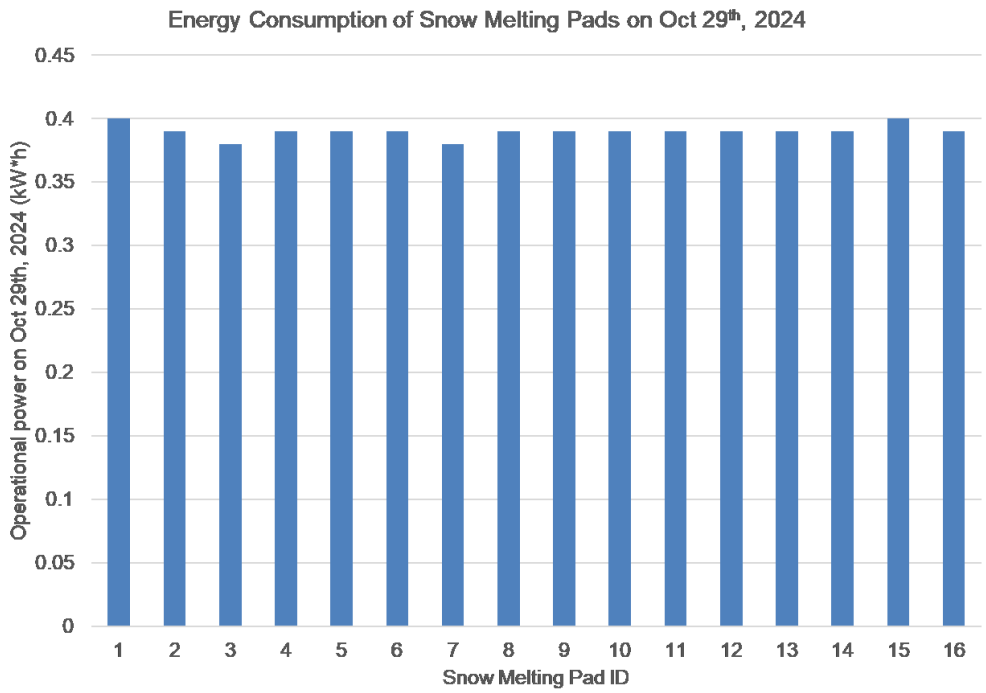

Figure 5.13 Daily avaerge power consumption of the 16 snow melting pads.

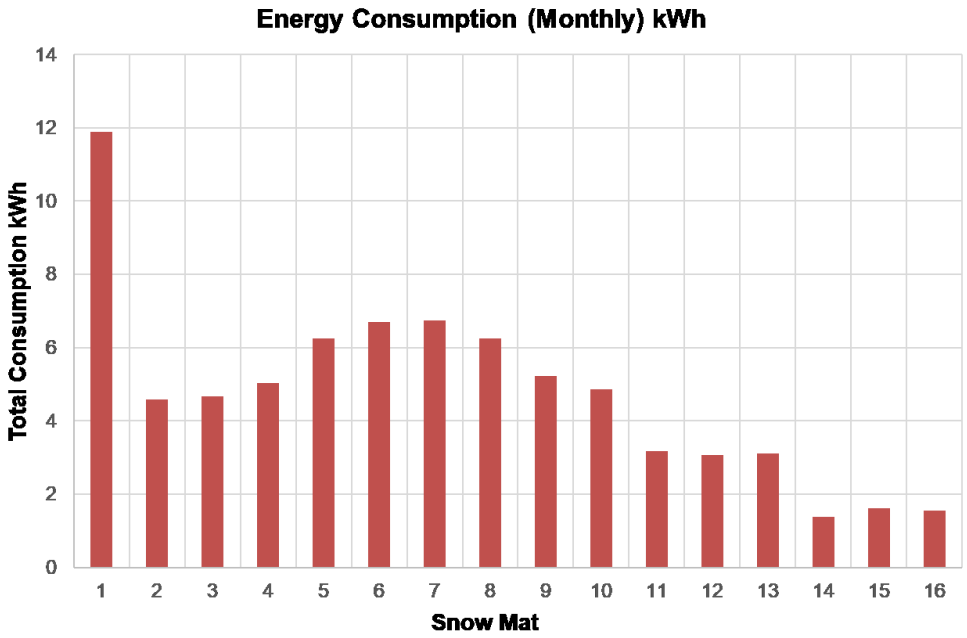

Figure 5.14 Monthly power consumption of the 16 snow melting pads in February 2025.

5.2.2.1 Snow melting

Snow melting has been proven to be a viable path to consume the energy generated and render the solar snow fence to be an active snow drift control with infinite reservoir capacity. During the 2024-2025 winter season, a clear path formed by the snow melting pads is shown in Figure 5.15 and Figure 5.16. A close view of the snow melting pads and the drifted snow profile is shown in Figure 5.17.

Figure 5.15 The clear walkway path formed by the 16 snow melting pads in October 2024.

Figure 5.16 The clear walkway path formed by the 16 snow melting pads in November 2024.

Figure 5.17 A close view of the snow melting pad and the drift profile formed in January 2025.

Chapter 6: Conclusions and final memorandum on research benefits and implementation steps

6.1 The research benefits of the solar snow fence system

6.1.1 Improve the life-cycle cost of structural snow fences.

Structural snow fences are a critical component of highway accessories. Solar snow fences serve snowdrift control and produce green energy, which can offset the initial investment of traditional structural snow fences and motivate their large-scale implementation. From the data collected in the field, it was confirmed that the 100-ft solar snow fence could produce 10-30 kW*h per day depending on how many sunny days there were in a month, which is close to one average household's power use. The energy data in August and September was less because the data collection system was in the testing stage and on and off during its operation. Based on the actual investment made in the 100-ft solar snow fence, the payback period was about 11 years. However, the project's scalability will play a crucial role. For larger-scale endeavors, like those extending to 1 mile, economies of scale could significantly lower costs and improve economic efficiency, potentially shortening the payback period to 5 years.

6.1.2 Safety

Snowdrifts can pose a significant threat on roadways. Snow fences reduce snowdrifts and snow removals and keep roadways in good clean condition, which leads to a reduced traffic accident rate and saves people's properties and lives. Based on the traffic accident data collected by UsDOT, 4% accidents of vehicle crashes are snow or ice-related; more than 1,300 people are killed in car crashes in the snow or ice every year, and more than 116,800 people are injured in vehicle crashes on snowy, slushy, or icy pavement annually. Based on the snowdrift data collected from the 100-ft solar snow fence, the drifting control of the solar snow fence was better than the traditional snow fence due to its better rigidity. The solar snow fence was made into an active snow fence system through snow melting with the electricity generated, which enhances the solar snow fence storage capacity tremendously (near infinity).

6.1.3 Technology development

This project developed an integrated energy-harvesting solar snow fence system along roadways, a new technology that can produce green energy, does not occupy additional land, and is easy to construct. With these components designed in detail on record, from the helical piling construction, the aluminum frame of solar strips, quick connection between posts and solar frame, remote electrical monitoring, to self-protected controllers and converters, the technology was field-implemented successfully in this project and is ready to be extended to other states when possible.

6.2 Implementation guide

Following the implementation steps adopted in this project, an implementation guide was summarized as follows:

I. Prepare the land for construction. Dry and roughly leveled land is preferred. Minimal preparation is needed.
II. Purchase the solar strips (preferred dimensions are 144x6x1/8 or 144x6x3/8. Potential vendors are Silicon Solar (www.siliconsolar.com) and Lishui E-able Power Equipment Co. LTD (sales@e-ablepower.com).
III. Purchase the T-slotted aluminum bar and aluminum brackets from McMaster-Carr (https://www.mcmaster.com/47065T101/) and West Side Steel (Tel: 701-365-8511) at Fargo for the aluminum plates.
IV. Cut the T-slotted aluminum bar into 6’ and 6'' long and cut aluminum plates into the dimensions shown in Figures 1.1 and 1.2 through hydro-cutting at the NDSU mechanical lab.
V. Assemble the solar strips into the T-slotted aluminum frame and the connection bracket (Figure 1.1 and Figure 1.2).
VI. Ship helical piles and the fence posts with pre-made 3/8’’ connection holes 1’ apart from each other and the helical drill machine to the site (vendor: www.technoMetalPost.com). The helical piles are P3-16 type, with 6’ underground. The fence posts are also P3-16 type and 8’ in length.
VII. Start the piling process. After the piling process is completed, connect the above-ground post with the underground pile through welding.
VIII. Connect the solar strips to the posts through U-bolt connections following the installation drawing in Appendix A.
IX. Install the host cabinet for batteries, chargers, and inverters. Sixteen batteries, 4 chargers, and 1 inverter are needed. One charger is used for 4 batteries to provide 12 volts and 14 Amps input. One solar module (two spans of 7 solar strips) is connected with one charger and supplies the energy to charge the 4 batteries. A total of 4 modules are used for the solar snow fence implemented. The batteries are from Renogy Deep Cycle AGM Battery with a capacity of 12 Volt and 200Ah. The charger is the 80 Amp MPPT Solar Charge Controller from AMPINVT with 48V, 36V, 24V, or 12V inputs. The inverter is from XYZ INVT with a capacity of 8000w and converts 24v DC to 110v AC. The converted AC power is used by the monitoring and the snow-melting system.
X. Connect the wires of the solar system with the batteries, chargers, and inverters following Figures 3.2 and 3.3.
XI. Connect the output power with the snow melting pads or other uses.

References

1. Federal Highway Administration. (2016). *Renewable energy generation in the highway rights-of-way* (FHWA-HEP-16-052). Washington, DC: FHWA.
2. Federal Highway Administration. (2017). *Highway renewable energy: Photovoltaic noise barriers* (FHWA-HEP-17-088). Washington, DC: FHWA.
3. Oregon DOT. (2016). *Solar highway program: From concept to reality: A guidebook for departments of transportation to develop solar photovoltaic systems in the highway rights-of-way*. Salem, OR: Oregon DOT.
4. Carder, D. R. & Barker, K. J. (2006). *M27 trial of highway noise barriers as solar energy generators* (TRL limited report PPR178). Winchester, UK: Transport Research Laboratory (Great Britain), Great Britain Highways Agency.
5. Morgan, P.A. (2006). *Photovoltaic noise barriers: Scope for demonstration schemes on London's main roads* (TRL limited report PPR128). London: Transport Research Laboratory (Great Britain), Greater London Highways Agency.
6. Vanhooreweder, B., Marcocci, S., & De Leo, M., (2017). *State of the art in managing road traffic noise: Noise barriers*. Paper presented at the conference of European Directors of Roads, Brussels, Belgium.
7. Klingner, R. E., McNerney, M. T.,& Busch-Vishniac, I. J. (2003). *Design guide for highway noise barriers* (No. 1471-1474). Austin, TX: Center for Transportation Research, Bureau of Engineering Research, University of Texas at Austin.
8. Tabler, R. D. (2003). *Controlling blowing and drifting snow with snow fences and road design* (No. NCHRP Project 20-7 (147). Washington, DC: The National Academies, The American Association of State Highway and Transportation Officials.
9. Constantinescu, G., Muste, M., & Basnet, K. (2015). *Optimization of snow drifting mitigation and control methods for Iowa conditions* (TR-626 Report). Ames, IA: Iowa State Department of Transportation.
10. ETSC. (1995). *Reducing traffic injuries resulting from excess and inappropriate speed*. Brussels: European Transport Safety Council.
11. Scrapmonster. (n.d.). *Steel scrap prices USA, UK, China, India, current scrap steel price*. Retrieved from https://www.scrapmonster.com/scrap-prices/category/Steel/300/1/1
12. Yang, M., Yu, Y., & Cao, D. (2021). Harnessing solar energy through noise barriers and structural snow fencing (No. MN 2021-20). St. Paul, MN: Minnesota. Department of Transportation.
13. NREL. (2016a). *Using power purchase agreements for solar deployment at universities.* Retrieved from https://www.nrel.gov/docs/gen/fy16/65567.pdf
14. TruNorth Solar. (n.d.). *Federal solar investment tax credit (ITC)*. Retrieved from https://www.trunorthsolar.com/incentives/#:~:text=In%202020%2C%20the%20tax%20credit,will%20end%20in%20January%202023.
15. Minnesota Department of Commerce (MnDOC), Division of Energy Resources. (2019). *Minnesota renewable energy standard: Utility compliance*. Retrieved from https://www.leg.mn.gov/docs/2019/mandated/190330.pdf
16. NREL. (2012) *Photovoltaic degradation rates – An analytical review.* Retrieved from https://www.nrel.gov/docs/fy12osti/51664.pdf
17. Pvwatts. (n.d.). *Pvwatts calculator*. Retrieved from https://pvwatts.nrel.gov/pvwatts.php

18. U.S. Environmental Protection Agency (EPA). (n.d.). *Greenhouse gas equivalencies calculator*. Retrieved from https://www.epa.gov/energy/greenhouse-gas-equivalencies-calculator
19. NREL. (2016b). *The role of advancements in solar photovoltaic efficiency, reliability, and costs.* Retrieved from https://www.nrel.gov/docs/fy16osti/65872.pdf
20. NREL. (2018a). *U.S. solar photovoltaic system cost benchmark: Q1 2018.* Retrieved from https://www.nrel.gov/docs/fy19osti/72399.pdf
21. Taxmaps. (n.d.). *Arcgis web application*. Retrieved from https://taxmaps.state.mn.us/salestax/
22. Enbar, N., Weng, D., & Klise, G. T. (2016). *Budgeting for solar PV plant operations & maintenance: Practices and pricing* (No. SAND-2016-0649R). Albuquerque, NM: Sandia National Lab.
23. Fthenakis, V. M. (2000). End-of-life management and recycling of PV modules. *Energy Policy, 28*(14), 1051–1058.
24. Guney, I., & Onat, N. (2010). *Cost calculation algorithm for photovoltaic systems*. Retrieved from https://www.intechopen.com/books/paths-to-sustainable-energy/cost-calculation-algorithm-for-photovoltaic-systems.
25. Federal Reserve. (2024). Discount rate minutes - January 22 and 31, 2024. Retrieved from https://www.federalreserve.gov/newsevents/pressreleases/files/monetary20240227a1.pdf
26. NREL. (2018b). *2018 U.S. utility-scale photovoltaics-plus-energy storage system costs benchmark*. Retrieved from https://www.nrel.gov/docs/fy19osti/71714.pdf
27. U.S. Department of Energy (DOE). (2021). *Investment tax credit requirements for privately owned solar photovoltaic systems on federal sites*. Retrieved from https://www.nrel.gov/docs/fy21osti/79936.pdf
28. U.S. Environmental Protection Agency (EPA). (2014). *Emission factors for greenhouse gas inventories*. Retrieved from https://www.epa.gov/sites/production/files/2015-07/documents/emission-factors_2014.pdf
29. U.S. Energy Information Administration (EIA). (n.d.). *EIA - Independent statistics and analysis*. Retrieved from https://www.eia.gov/energyexplained/units-and-calculators/energy-conversion-calculators.php
30. U.S. Environmental Protection Agency (EPA). (2017, January 9). *The social cost of carbon*. Retrieved from https://19january2017snapshot.epa.gov/climatechange/social-cost-carbon.html
31. Fan, J. (2014). *Life cycle assessment and life cycle cost of photovoltaic panels on Lake Street parking garage* (doctoral dissertation), Colorado State University, Fort Collins, CO.
32. Ernie's Wagon. (n.d.). *Fence removal service*. Retrieved from https://www.ernieswagon.com/fence-removal/
33. FHWA. (n.d.) *Noise barrier inventory tool*. Retrieved from https://www.fhwa.dot.gov/environment/noise/noise_barriers/inventory/inventory_tool/index.cfm#results
34. VTPI. (2016) *Transportation cost and benefit analysis techniques, estimates and implications*. Retrieved from https://www.vtpi.org/tca/
35. MnDOT(a). (n.d.) *Roadway data – Fun facts*. https://www.dot.state.mn.us/roadway/data/fun-facts.html
36. Morgan, S. M., Kay, D. H., & Bodapati, S. N. (2001). Study of noise barrier life-cycle costing. *Journal of Transportation Engineering, 127*(3), 230–236.
37. AcreValue. (n.d.). *AcreValue web application*. Retrieved from https://www.acrevalue.com/map/MN/?lat=46.521455&lng=-93.36421&zoom=5

38. MN House Research. (2019). *Property tax 101: Property tax variation by property type*. Retrieved from https://www.house.leg.state.mn.us/hrd/pubs/ss/ssptvart.pdf
39. MN Department of Revenue. (n.d.). *State general property tax*. Retrieved from https://www.revenue.state.mn.us/state-general-property-tax#:~:text=The%20final%20commercial%2Dindustrial%20state,taxes%20payable%202021%20is%2017.306%25
40. Clay County MN. (n.d.). *Tax capacities & rates*. Retrieved from https://claycountymn.gov/163/Tax-Capacities-Rates
41. MnDOT(b). (n.d.). *Living snow fences – Control blowing and drifting snow*. Retrieved from http://www.dot.state.mn.us/environment/livingsnowfence/forms.html
42. MnDOT(c). (n.d.). *Example – MnDOT's blowing snow control annual payment*. Retrieved from https://www.dot.state.mn.us/environment/livingsnowfence/pdf/payment-sched-example.pdf
43. Minnesota Department of Labor and Industry. (2019). *Solar photovoltaic system and the state building code*. Retrieved from https://www.dli.mn.gov/sites/default/files/pdf/fs_code_solar.pdf
44. Federal Aviation Administration. (2018). *Technical guidance for evaluating selected solar technologies on airports.* Retrieved from https://www.faa.gov/airports/environmental/policy_guidance/media/FAA-Airport-Solar-Guide-2018.pdf
45. FHWA. (2016). *Renewable energy generation in the highway right-of-way*. Retrieved from https://www.fhwa.dot.gov/real_estate/publications/row/fhwahep16052.pdf
46. NREL. (2010). *Insuring solar photovoltaics changes and possible solutions*. Retrieved from https://www.nrel.gov/docs/fy10osti/46932.pdf
47. Office of the Federal Register (OFR) and the Government Publishing Office. (n.d.). *Electronic code of federal regulations*. Retrieved from https://www.ecfr.gov/cgi-bin/text-idx?SID=3c25c40ead77be4e7bf7442e1ea6518b&mc=true&node=pt23.1.645&rgn=div5#sp23.1.645.b
48. Kurze, U. J., & Anderson G. S. (1971). Sound attenuation by barriers. *Applied Acoustics, 4*(1), 35–53
49. Ashton, S. J., & Mackay, G. M. (1979). *Some characteristics of the population who suffer trauma as pedestrians when hit by cars and some resulting implications*. Proceedings of the 4th IRCOBI conference, Gothenburg, 39-48.

Appendix A: Implementation drawing of the solar snow fence

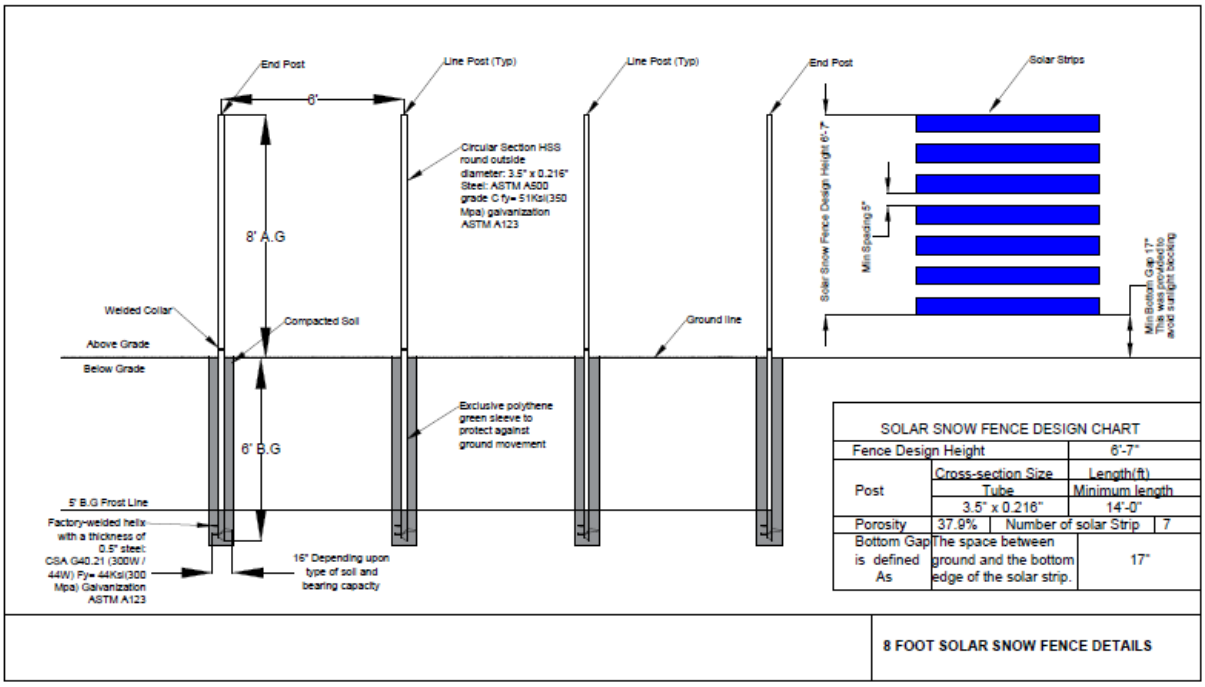

Figure A-1 Implementation drawing of the solar snow fence